Analytical Modeling of IEEE 802.11-Type CSMA/CA Networks With Short Term Unfairness

Abhijit Bhattacharya and Anurag Kumar, *Fellow, IEEE*

***Abstract*— We consider single-hop topologies with saturated transmitting nodes, using carrier-sense multiple access with collision avoidance (CSMA/CA) for medium access, as standardized under the IEEE 802.11 distributed coordination function. We study systems where one or more backoff parameters of the CSMA/CA protocol (the initial backoff, the backoff multiplier, and the number of retries) are different from the standard. It is known that, for several classes of these protocol parameters, such systems exhibit a certain performance anomaly known as short term unfairness. We also find that the phenomenon of short term unfairness is observed in systems where the propagation delays among the participating nodes are not negligible compared with the duration of a backoff slot, even when the nodes use the default backoff parameters of the standard. It also turns out that the standard fixed point analysis technique (and its simple extensions) does not predict the system behavior well in such cases. For systems with large propagation delays, we observe that, as propagation delay increases, the collision probability of a node initially increases, but then flattens out, contrary to what is predicted by the standard fixed point approximation. Our study of several example systems reveals some interesting connections between the protocol parameters, the number of nodes, the propagation delay, and the degree of unfairness. This paper reveals that the inability of the standard fixed point model to capture the performance in such cases is due to its state-independent attempt rate assumption. In this paper, we develop a novel approximate, but accurate, analysis that uses state-dependent attempt rates with a parsimonious state representation for computational tractability. The analytical method is also able to quantify the extent of short term unfairness in the system, something not possible with existing analytical techniques, and can, therefore, be used to tune the protocol parameters to achieve desired throughput and fairness objectives.**

***Index Terms*— Wireless LAN, unmanned aerial vehicles, stochastic processes, Markov processes.**

I. Introduction

THE most popular performance analysis of IEEE 802.11 CSMA/CA (WiFi) networks was provided by Bianchi in the seminal work [1], and was later generalized by Kumar *et al.* [2]. However, it is now well-known that this analysis might not work if the DCF backoff parameters are different from those in the standard; in particular, Ramaiyan *et al.* [3] demonstrated via some examples that the analysis may not capture the system performance well when the backoff sequences are such that the system exhibits short-term unfairness. In these examples, one node or the other repeatedly succeeds in acquiring the channel for a long random time period, while the other nodes languish at large backoff durations, followed by another, randomly selected node acquiring the privileged status, and so on. In Section IV, we present such an example of short term unfairness with parameters that arise in extensions of the IEEE 802.11 standard (i.e., the IEEE 802.11e standard). Further, we have found that the phenomenon of short-term unfairness is also observed under the practical setting where the backoff sequences are as per the standard, but the *propagation delays* among the participating nodes are large compared to the duration of a backoff slot; this situation arises in a variety of applications such as providing broadband connectivity to remote rural areas using WiFi based *long distance* networks [4]. There has also been interest in using WiFi for network formation among Unmanned Aerial Vehicles (UAVs), or between UAVs and a ground station over distances of several kilometres. Furthermore, with the evolution of WiFi standards, the slot (i.e., backoff slot) durations are decreasing; e.g., the WiFi standard IEEE 802.11ac adopts a slot duration of 9 μs, as compared to 20 μs in the older IEEE 802.11b. Thus, even the propagation delays that were negligible compared to the slot duration in earlier WiFi standards may occupy multiple slot durations in the future. In this case also, the analysis in [1] (or simple extensions thereof) does not work well.

The analysis of [1] and [2] makes the key modeling simplification that, in steady state, during contention periods, the nodes make attempts as *equal rate* independent Bernoulli processes embedded at the backoff slot boundaries. *Since the node attempt model is state-independent, such a model does not capture the possibly advantageous position that a successful node might be in, as compared to the unsuccessful nodes, and hence cannot yield the short term unfairness that has been observed in the situations described earlier.* This significantly limits the applicability of the approximation in [1] and [2], as there is no way without an exhaustive simulation to know whether the approximation will predict the system performance correctly for a given set of parameters. The DCF mechanism is finding its way to newer applications beyond the WLAN standards, and a common engineering practice for new applications is to tune the parameters of the protocol to the needs of the particular application; even EDCF uses the initial backoff and the backoff multiplier to create service differentiation [5].

Manuscript received October 23, 2016; revised May 28, 2017; accepted August 10, 2017; approved by IEEE/ACM TRANSACTIONS ON NETWORKING Editor G. Paschos. Date of publication September 27, 2017; date of current version December 15, 2017. *(Corresponding author: Abhijit Bhattacharya.)*

A. Bhattacharya was with the Department of Electrical Communication Engineering, Indian Institute of Science, Bangalore 560012, India. He is now with Qualcomm Research India, Bangalore 560066, India (e-mail: abhijitb@qti.qualcomm.com).

A. Kumar is with the Department of Electrical Communication Engineering, Indian Institute of Science, Bangalore 560012, India (e-mail: anurag@ece.iisc.ernet.in).

This paper has supplementary downloadable material available at http://ieeexplore.ieee.org, provided by the authors.

Digital Object Identifier 10.1109/TNET.2017.2747406

It is, therefore, necessary to have an analytical technique that can predict the system performance not just for the standard protocol parameters, but for more general backoff parameters, as well as with propagation delays. Our work is intended as a first step in that direction. In this work, we address this problem for the case of a single-hop topology consisting of *saturated* transmitting nodes and their receivers, using the IEEE 802.11 DCF basic access mechanism for medium access. We use the theory of Markov Regenerative Processes to develop a tractable generalization of the analysis in [1]. Comparison against extensive simulations have shown that the analysis captures the system performance well even in the presence of high correlation in system evolution.

Summary of Contributions: Based on a study of the evolution of the system, and a stochastic simulation, we find that the phenomenon of short term unfairness in IEEE 802.11 DCF networks renders inaccurate the stateless, constant attempt rate approach adopted in [1] and [2]. In addition, our studies also reveal some interesting connections between the extent of unfairness, the system size, and the protocol parameters (see Section IV). In our analytical approach, we maintain some state information, and introduce state-dependent attempt rates. How we do this in a parsimonious and computationally tractable manner, while developing an accurate approximation, is the primary contribution of this work (Section VII). Moreover, we demonstrate a key property of systems with large propagation delays, namely, misaligned sensing of channel idleness, that sets them apart from systems with negligible (zero) propagation delays. This has important consequences on the tractability of the analysis, which we discuss in Section VI-A.

A. Related Work

There is a considerable body of literature on performance analysis of IEEE 802.11 DCF, starting with the seminal work by Bianchi [1], which was later generalized by Kumar *et al.* [2] to incorporate general backoff parameters. Several extensions have been proposed since then to account for non-saturated nodes, and/or hidden terminals, among others. See, for example, [6], [7]. Performance analysis of IEEE 802.11e EDCA has also received significant attention; see [3], [8], and the references therein. However, none of this work is suitable for predicting the performance of systems that exhibit short term unfairness, and this has been explicitly pointed out in [8].

Short term as well as long term unfairness have been observed (and modeled) before in the presence of *hidden terminals* in WLANs, e.g., by Garetto *et al.* [9]. However, parts of their analysis rely on the assumption that under no hidden nodes, the system is fair, and existing techniques predict system behavior accurately, which is not quite correct as demonstrated in [3], and also our current work. Therefore, in the light of the findings in our current work and in [3], the problems in [9] need a relook.

Simo-Reigadas *et al.* [10] aimed to develop an extension of the analysis in [1] to predict the performance of IEEE 802.11 DCF with non-negligible propagation delays. However, we shall argue in Section V-B that the analysis in [10] *does not capture two distinct features of such systems*, and as a consequence, the *collision/success probabilities computed using the analysis are inaccurate compared to simulation results* obtained from a detailed stochastic model, as well as from the Qualnet simulator [11].[1]

Vlachou *et al.* [12] modeled IEEE 1901 CSMA/CA protocol used in Power-Line Communication (PLC) networks, and observed short-term unfairness in such systems. However, due to important differences between IEEE 1901 CSMA/CA and IEEE 802.11 CSMA/CA protocols as also pointed out in their work, their techniques cannot be applied to IEEE 802.11 DCF.

Our work is thus intended as a first step towards an accurate analytical model for such systems. Our key contribution is the development of a principled approach for analyzing IEEE 802.11 DCF based systems with short term unfairness.

II. A Brief Description of IEEE 802.11 DCF

As in [1], we make the following assumptions throughout the paper: the nodes perform basic access without RTS-CTS. There are no hidden nodes, and there is perfect sensing of an ongoing transmission. The transmission queues are saturated, i.e., each node always has a packet to transmit. There are no channel errors. In case of simultaneous transmission by multiple nodes, there is no packet capture.

The backoff durations of the nodes are in multiples of a standardized *backoff slot* (e.g., 20 μs in IEEE 802.11b). When a node completes its backoff, it starts a packet transmission. In the zero propagation delay setting, any other node that does not complete its backoff simultaneously hears the ongoing transmission instantaneously, and freezes its backoff counter. If no other node completes its backoff simultaneously, the packet transmission is successful, and the intended receiver sends a MAC level ACK. On the other hand, if two or more nodes complete their backoffs together, they all start a packet transmission simultaneously, leading to a collision. At the end of the activity duration (successful transmission or collision), each transmitter involved in the activity samples fresh backoffs. All the nodes wait for an interval called DIFS, and resume counting down their backoffs thereafter. If a packet encounters several successive transmission failures, the packet is discarded; in the saturated queue model the discarded packet is immediately replaced with another packet.

In the IEEE 802.11 framework, each node samples its backoff uniformly from a contention window $[1, W_k]$, where W_k is the contention window size after the k^{th} reattempt, $0 \leq k \leq K$; K is the maximum number of reattempts after which a packet is discarded. After each reattempt, the contention window size is increased by a factor p, i.e., $W_{k+1} = pW_k$, until it reaches a maximum allowed value. After a successful transmission, the contention window is reset to W_0. For example, in the IEEE 802.11b standard, $W_0 = 32$, $p = 2$, $K = 6$, and the maximum allowed contention

[1]This anomaly does not show up significantly in the numerical results presented in [10] primarily because they *do not compare the collision/success probabilities obtained from their analysis against any experimental or simulation results*, and provide comparison results only for system throughput, which, as our numerical results later on demonstrate, is *less sensitive to* (but not unaffected by) inaccuracies in the analysis than other performance measures such as collision probability.

window size is 1024. Throughout this work, we shall assume a *homogeneous* system, i.e., all the nodes have the same backoff parameters.

III. IEEE 802.11 DCF Modeling in [1] and [2]

The system evolution over backoff slots can be modeled as a Discrete Time Markov chain (DTMC) that tracks the backoff stage and the residual backoff of each node at the beginning of each backoff slot; see [2]. However, the state space of this DTMC is too large to facilitate a direct computation; hence approximate analytical techniques were developed to predict the system performance with reasonable accuracy.

A. The Approximate Analysis in [1] and [2]

The Decoupling Approximation: Consider n contending transmitters. From the description of the protocol, it is clear that the system alternates between transmission and contention periods, and that the attempt processes of the nodes are *dependent*. *The decoupling approximation is to assume that during the contention periods, the attempt processes of the nodes are independent Bernoulli processes with equal attempt rate,* β. Let γ denote the collision probability: i.e., the probability that an attempt by a tagged node finds simultaneous attempts by other nodes. Using this approximation, in [2] the backoff process evolution at a tagged node is analyzed via a renewal-reward analysis, with renewal points being the successful transmission or packet discard epochs. This yields $\beta := G(\gamma)$, where

$$G(\gamma) := \frac{1+\gamma+\gamma^2+\cdots+\gamma^K}{b_0+\gamma b_1+\gamma^2 b_2+\cdots+\gamma^k b_k+\cdots+\gamma^K b_K} \quad (1)$$

Here, b_k is the mean backoff duration after the k^{th} reattempt, i.e., $b_k = (1+W_k)/2$ slots. Using the Bernoulli attempt process approximation, the collision probability, γ, is given by

$$\Gamma(\beta) := 1-(1-\beta)^{(n-1)} \quad (2)$$

These two equations together constitute the desired fixed point equation.

Remarks:

1) It was shown in [2] that $\Gamma(G(\gamma)) : [0,1] \to [0,1]$, has a unique fixed point if $b_k, k \geq 0$, is a nondecreasing sequence, which is, in fact, the case for the IEEE 802.11 standard.

2) The asymptotic mean field analysis in [13], with its conclusion of "convergence to chaos," has been suggested as supporting the idea of the decoupling approximation. Hence, in the remainder of the paper, we will refer to the analysis in [1] and [2] as the mean field analysis. □

IV. A System With Short Term Unfairness

Our point of departure from the above work is the following question: will the mean field type analysis ([1], [2]) continue to predict the system performance well, if the protocol parameters are changed from those in the IEEE 802.11 standard? *In particular, will it work for any* non-decreasing *backoff sequence* $(b_0,\ldots,b_K)$ *(recall from Section III that the system 1 and 2 has a unique fixed point for non-decreasing backoff sequences), and any number of nodes,* n*?* It turns out that this is not the case.

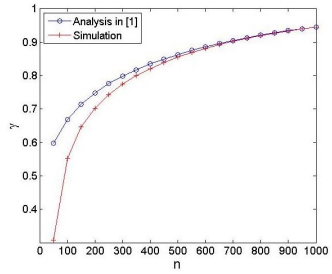

Fig. 1. Collision probability vs. number of nodes for the backoff sequence of Section IV-A; comparison of the values obtained from the analysis in [1] against those obtained from simulations.

A. Example: An IEEE 802.11-Like Backoff Expansion Framework (Adapted From [3])

Consider a system where all nodes use the IEEE 802.11 DCF backoff expansion framework for medium access, but with parameters as follows: $K = 7$, $b_0 = 1$, $b_k = 3^k b_0$ for all $0 \leq k \leq K$. This system is of interest because it is in the framework of IEEE 802.11e standard, which allows modification of the backoff parameters for service differentiation purpose (see, for example, [5] and [14, Ch. 5]).

Figure 1 demonstrates the performance of the analysis in [1]. The error in the collision probability obtained from the analysis in [1] is much worse than 10% when the number of nodes, n, is less than 100. For the parameters in the standard, the mean field analysis worked remarkably well, yielding estimates of the collision probability that were within 3-4% of the values obtained from simulation ([1], [2]). Thus, in the remainder of the paper, we will use an error of more than 10% as an indication of the mean field analysis being unsuitable for modeling the system.

To understand why the mean field analysis does not capture the system performance, let us take a closer look at the system behavior for a small value of n. Consider a system with $n = 20$ nodes, and backoff parameters as above. It turns out that this system exhibits *short term unfairness*, in the sense that when a node's transmission is successful, it monopolizes the channel for the next several thousands of backoff slots, resulting in starvation and high short term collision probabilities for the other nodes [3].

Panel 1[2] of Figure 2 depicts the short term collision probabilities of two of the 20 transmitters. We recall that this contention based system alternates between *channel activity periods* (during which one or more node transmits a packet) and *contention periods* during which the nodes count down their backoff counters. We call a contention period along with the following channel activity period a *transmission cycle*. Each point in the plot is the short term collision rate (i.e., the ratio of the number of collisions to the number of attempts) of a node over a window of 200 consecutive transmission cycles. The results are shown for 100 windows in the simulation. Also plotted is the long run average collision probability,

[2]When discussing figures with multiple panels, in the text we will number the panels row-wise, from left to right

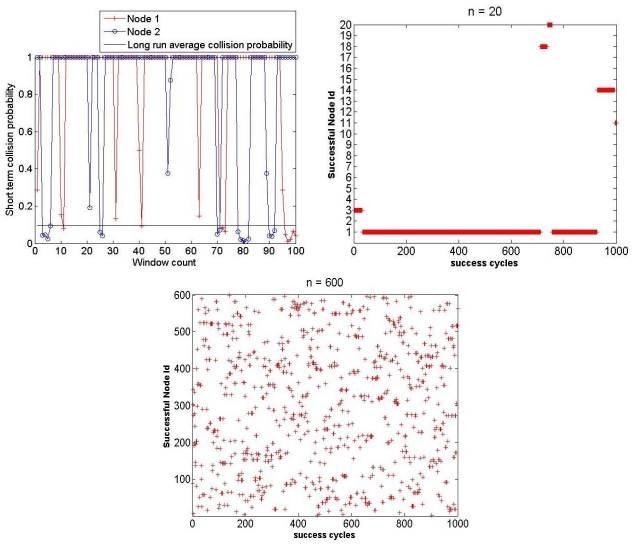

Fig. 2. Simulation results depicting short term unfairness for the backoff sequence in Section IV-A. Panel 1 shows the short term collision probabilities of two of the transmitters (see text for details) for a system with $n = 20$; also plotted is the long run average collision probability, averaged over all the nodes and all simulation time. Panels 2 and 3 show the evolution of the success process of the two nodes over 1000 successful transmissions of the system with $n = 20$ and $n = 600$ respectively. The success process is bursty for $n = 20$, indicating short term unfairness. The burstiness (and hence, short term unfairness) decreases as the number of nodes, n, increases.

averaged over all the nodes, and over the simulation duration. It can be observed from the plot that it is often the case that in a window of 200 transmission cycles where Node 1 has a low short term collision probability (often as low as 0.05), Node 2 has a very high short term collision probability (close to 1), and vice-versa, thus indicating that one of the nodes monopolizes the channel in each window, shutting out the other node, thus leading to a high collision probability for the other node during that period.

An alternate depiction of the short term unfairness in this 20-node system is shown in Panel 2 of Figure 2, where we show the Node IDs of the successful nodes for the last 1000 successful transmissions in a simulation run. Observe that the success processes at the nodes are bursty[3] in nature, indicating that one node captures the channel over prolonged durations, while the other gets zero throughput during that period.

Intuitively, the short term unfairness in this system can be explained as follows: when a node succeeds, it attempts again in the immediate next slot (since the initial backoff window is only 1 slot), whereas due to the much larger backoffs after successive collisions, the other nodes are busy counting down their large residual backoffs. This causes the successful node to monopolize the channel (attempt in every slot).

[3]This conclusion is reached by applying the Wald-Wolfowitz Runs test (see, e.g., [15]) for the null hypothesis that the sample is from a Bernoulli random process (as would be suggested by the Bernoulli attempt rate model in [1] and [2]). In every case where we conclude that the success process is bursty, the null hypothesis is rejected with a vanishingly low probability of false rejection, and in every case that we conclude that the success process is "fair", the null hypothesis could not be rejected even for false rejection level arbitrarily close to 1.

Short-Term Unfairness and Inaccuracy of the Mean Field Analysis: This also explains why the collision probability predicted by the analysis in [1] and [2] is higher than that obtained from simulations (see Figure 1). This is because in the presence of short term unfairness, the last successful node has a much larger probability of accessing the channel in the next slot than the other nodes, thus further boosting its success probability, unlike in a fair system, where all the nodes have comparable probability of accessing the channel, resulting in a higher probability of collision. *The mean field analysis ignores the correlation in the system evolution in an unfair system.* The high correlation in the system evolution means that the decoupling approximation made in the analysis in [1] and [2] does not hold, which explains why the analysis does not work.

Decreasing Short-Term Unfairness With Increasing n: Figure 2 also demonstrates the variation in short term unfairness as a function of the number of nodes, n (see Panels 2 and 3). It can be seen from Panel 3 that as the number of nodes becomes large, the burstiness in the success processes of the nodes disappears, implying fairer access to the channel for all the nodes, i.e., the short term unfairness disappears. This is consistent with the fact that the analysis in [1] (and the decoupling approximation) works well for larger n (see Figure 1).

The decrease in short term unfairness with increasing n can be intuitively explained as follows. The successful node goes to backoff stage 0, where it attempts again with probability 1 in the very next slot. The other nodes have large backoffs and hence the probability of any individual node attempting in the same slot as the successful node is small. However, if there are enough of the other nodes (i.e., n is sufficiently large) then the probability of one or more of them completing their backoffs in the next slot will be large, hence the probability of the successful node colliding in its next attempt can be large, thereby causing that node as well to quickly join the ranks of the nodes with large backoffs, thus ameliorating the unfairness.

See the techreport [16] for more examples of short term unfairness, reinforcing the above observations.

Next, we demonstrate that short term unfairness is observed even with the default protocol parameters, when the propagation delays among the nodes are large compared to the duration of a backoff slot.

V. Systems With Large Propagation Delays

Consider the transmitter-receiver configurations shown in Figure 3. Let the propagation delay between each pair of transmitters be Δ, that between each receiver and all the transmitters be Δ_r (e.g., in configuration (b) of Figure 3, the propagation delay from receiver R1 to both the transmitters T1 and T2 is Δ_r), and the duration of each backoff slot be σ. Let $m \stackrel{\triangle}{=} \lfloor \frac{\Delta}{\sigma} \rfloor$, i.e., m is the propagation delay among the transmitters in integer multiples of slots. Also let $m_r \stackrel{\triangle}{=} \lfloor \frac{\Delta_r}{\sigma} \rfloor$. When the propagation delays are negligible, $m = m_r = 0$.

A node's transmission will be heard by the other transmitting nodes after a propagation delay of m slots. We consider the setting where the packet duration, T, is much larger

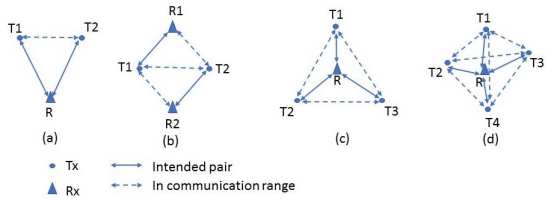

Fig. 3. Example systems with possibly large propagation delays where all transmitters are equidistant from one another, and each receiver is equidistant from all the transmitters. (a) 2 transmitters and 1 common receiver. (b) 2 transmitters, and 2 receivers. (c) 3 transmitters, with 1 common receiver at the centroid. (d) 4 transmitters, and 1 common receiver, in a tetrahedron configuration. Note that the transmitter configurations shown are the only possible ones under this restriction; however, additional receivers can be added in some cases, e.g., scenario (c).

than the propagation delay, m.[4] Thus, if two or more nodes finish their backoffs within m slots of one another, their transmissions collide, and all the packets involved are lost.

Upon a successful transmission, the transmitting node receives an ACK from its intended receiver. Due to the round-trip propagation delay between the transmitter and its receiver, the overall transmission overhead in a successful transmission is increased by $2m_r$ compared to the case without propagation delay. Thus, the ACK Timeout parameter in the protocol should be suitably adjusted for non-negligible propagation delays.

A. Short Term Unfairness

Panels 1 and 2 in Figure 4 depict snapshots of a simulation run for Scenario (b), Figure 3, operating with the standard protocol parameters of IEEE 802.11b, with a propagation delay of $m = m_r = 7$ slots. In Panel 1 of Figure 4, we depict 500 successive successful transmissions in the system, and the Node ID of the successful node in each of these transmissions. It is clearly seen from the plot that the success processes for the two transmitter-receiver pairs are bursty in nature; the burstiness is inferred in the same way as in Section IV-A.

To ascertain that this is not a sporadic phenomenon, but typical behavior of the system, we show in Panel 2 of Figure 4 the short term collision probabilities of the two nodes; each point in the plot is the short term collision probability of a node computed over a window of 100 consecutive system transmissions, and the process was repeated for 100 windows in the simulation. Also plotted is the long run average collision probability, averaged over all the nodes, and the simulation duration. We see from the plots that it is often the case that in a window where Node 1 has a low short term collision probability (often as low as 0.1), Node 2 has a very high short term collision probability (close to 1), and vice-versa, thus indicating that one of the nodes repeatedly succeeds over a window of at least 100 transmission cycles, shutting out the other node, thus leading to a high collision probability for the other node during that period.

In order to demonstrate that this property is observed only at higher propagation delays, we show in Panels 3 and 4

[4]This assumption is satisfied in most scenarios of interest. For example, if the PHY layer rate is 2 Mbps, the packet duration for a 1500 bytes packet is 6000 μs, whereas the propagation delay over a distance of 42 km is only 140 μs.

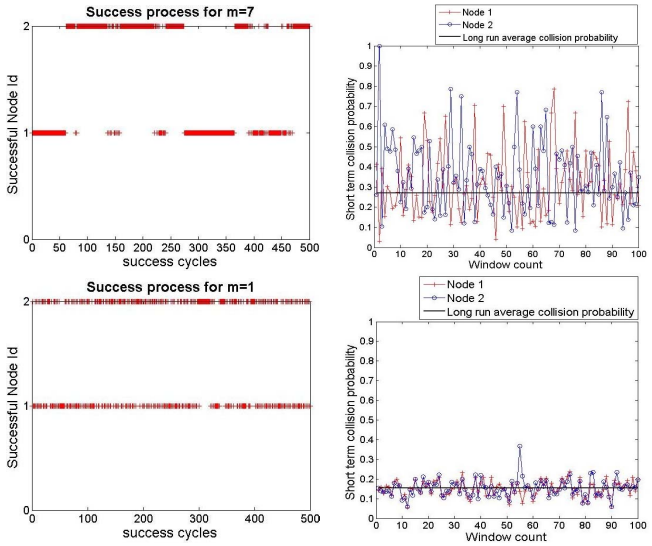

Fig. 4. Simulation results depicting short term unfairness at higher propagation delays for a system with 2 transmitting nodes, each having the default DCF backoff parameters. (Panels are row-wise, from left to right) Panels 1 and 2: Propagation delay between node pairs is $m = m_r = 7$ slots. Panel 1: Evolution of the success process of the two nodes over 500 successful transmissions of the system. Panel 2: Short term collision probabilities of the two transmitters; also plotted is the long run average collision probability, averaged over nodes and simulation duration. Panels 3 and 4: The same plots as in Panels 1 and 2, but for propagation delay $m = m_r = 1$ slot.

in Figure 4, snapshots of a simulation run for the same system as before, but with a propagation delay of $m = m_r = 1$ slot. It is observed from Panel 3 of Figure 4 that the success processes of the two nodes are no longer bursty in nature; in particular, no node is starved for a prolonged duration. From Panel 4 of Figure 4, we see that the large differences of short term collision rates between the two nodes are now absent.

Discussion: The phenomenon of short term unfairness with higher propagation delays stems from the fact that, with high propagation delay, the collision probability becomes very large (almost 30% beyond $m = 3$; see the γ plot in Figure 11) *even for a small number of nodes*, and so backoff distributions become stochastically very large as well. As a consequence, after a successful transmission, the residual backoffs of the frozen nodes are likely to be large. Since the successful node will sample its next backoff from the initial (smallest) window, its next backoff is likely to be much smaller than the other nodes. Thus, the successful node is likely to attempt much earlier than the other nodes, and succeed again; the number of other nodes that have large residual backoffs is small, making it unlikely that one of them will make an attempt and thereby dislodge the successful node.

B. Performance of an Existing Fixed Point Analysis for Large Propagation Delays

Simo-Reigadas *et al.* [10] aimed to develop an approximate analytical model for single-hop, long distance WiFi systems by extending the model in [17]. For the case of a homogeneous system, their model reduces to the following: each node, conditioned on being in backoff, attempts independently with a probability β in each slot, irrespective of the system state. When a node transmits, the conditional probability that its

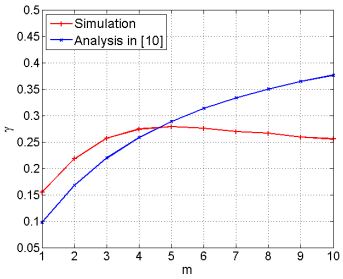

Fig. 5. Comparison of the analysis in [10] with simulation. Collision probability, γ, vs. m for Scenario (b) in Figure 3 with $\Delta = \Delta_r$.

transmission encounters a collision, is γ, independent of the system state. They obtain β in terms of γ using the well-known polynomial ratio formula (see Eqn. 1). To obtain the collision probability, γ, they observe (inaccurately) that the vulnerable window of a tagged node has size $2m$, since any node attempting within m slots before or after the tagged node's attempt will cause a collision. They then compute the probabilities of any node attempting in that vulnerable window by assuming (inaccurately) that the node was in backoff at the start of the vulnerable window, and using the Markov chain model proposed in [17] that describes the evolution of the node *in backoff time*. Thus, they arrive at a fixed point equation in γ.

The model in [10] *does not consider the fact that after a collision, due to the propagation delay, the starts of the backoff counters of the nodes could be misaligned* (see Section VI-A), and hence when a tagged node attempts again, its vulnerable window need not be $2m$, since the other nodes may not even have started their backoff countdowns. Moreover, the assumption of constant attempt probability β irrespective of the system state *ignores the short term unfairness property*, which has the effect of skewing the attempt probability in favor of a successful node as explained earlier. Figure 5 compares the collision probabilities obtained from the analysis in [10] against those obtained from simulations for the configuration (b) of Figure 3 with default backoff parameters of IEEE 802.11b, and a range of propagation delays. As can be seen, the values predicted in [10] do not match well with the simulation results.

Discussion and Proposed Way Forward

Our aim is to develop an accurate analytical technique to predict the performance of IEEE 802.11 systems that use general backoff prameters, and that have propagation delays. To that end, we adopt the following approach:

1. We first demonstrate a key property of systems with large propagation delays that sets them apart from systems with zero propagation delays, and discuss its implications. This property was not captured in the analysis in [10].

2. Recall from [2] that there is a $2n$-dimensional Markov chain model that *exactly* captures the system evolution for zero propagation delay. This model also holds for arbitrary backoff parameters (with zero propagation delay). The mean field type approximation developed in [1] and [2] is essentially an approximation for this Markov chain model. In Section VI, we show that for systems with possibly large propagation delays, there is a Markov renewal model that can be viewed as a generalization of the earlier $2n$-dimensional Markov chain model, and that *exactly* captures the system evolution. We use this model as a prototype for the system.

3. Simulation of this model is much faster compared to off-the-shelf even-driven simulators such as Qualnet [11], and allows us to examine certain finer details of the system performance with relative ease. Hence, in our subsequent simulations, we simulate this model.

4. However, analysis even of this model is computationally intractable. Hence, we introduce a parsimonious approximation of this Markov renewal model, which uses state dependent attempt rates to capture the bursty nature of the success processes due to short term unfairness (see Figure 4).

VI. A Markov Renewal Model of the System

In this section, we shall present a Markov renewal process model for the system evolution under possibly large propagation delays. We shall demonstrate via comparison with Qualnet simulations [11] (see Figure 8) that this model is indeed a faithful prototype for the system. Before presenting the model, we need to demonstrate a key property of systems with large propagation delays.

A. A Key Observation: Misaligned Sensing of Channel Idleness

In a system with zero propagation delay, all nodes sense the start and end of channel activity simultaneously, a DIFS period follows, and then the starts of the back-off periods at all the nodes are *always aligned*. In the present case, consider the situation depicted in the left panel of Figure 6 for a system with two transmitter-receiver pairs (for example, Scenario (b) in Figure 3). As explained in Figure 6, when Node 2 finishes its backoff within $k < m$ slots of Node 1, they encounter a collision, and *the starting points of when they next begin to count down their backoff counters are misaligned by k slots*. The misalignment, k, can take values in $\{0, 1, \ldots, m\}$.

Important Remarks on Misalignment:

1. The possible misalignment of the backoff counters happens *only when there is a collision*. In the case of a success, as explained in the right panel of Figure 6, they start their next backoff together.

2. *Note that in the case of a point-to-point link, there is a misalignment of the backoff counters of the two nodes by m_r slots even after a successful transmission. Hence, as such, we cannot apply the analytical model presented in this paper to a point-to-point link. However, only minor modifications to the state space are necessary to handle this case.*

3. Figure 6 can be drawn for more than two nodes being involved in a collision. Consider a multiple node collision, and denote by Nodes 1 and 2 respectively, *the node that attempted next to last, and the node that attempted last*. Then it is seen from the left panel of Figure 6 that Node 2 will start its backoff earlier than the other nodes, all of whom start their backoffs together. The misalignment is precisely the difference between the attempt instants of Nodes 1 and 2. *The general principle*

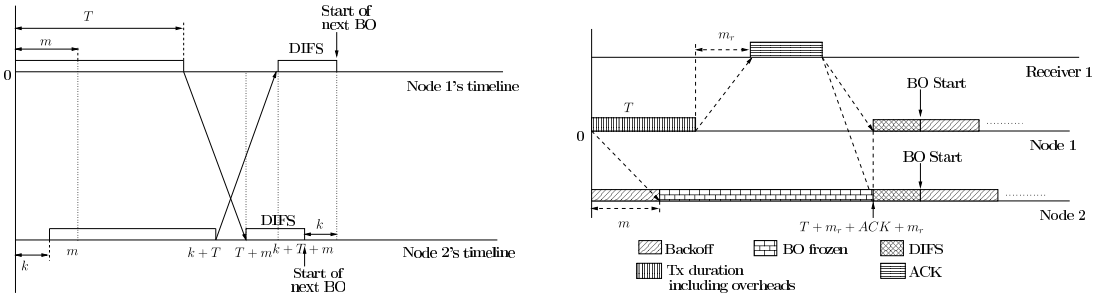

Fig. 6. **Left Panel: A collision, leading to misalignment**. Node 1 starts a transmission at time 0. Node 2 finishes backoff k slots after Node 1, where $k < m$, and starts its transmission, only to begin to sense Node 1's transmission at time m, thus resulting in a collision. Node 2 will sense the channel idle at time $T+m$, and count down its DIFS, after which, it will start a fresh backoff. However, Node 1 will sense the channel idle only at time $T+k+m > T+m$. Thus, Node 1 will start counting its DIFS k slots after Node 2, and hence it will also start its backoff countdown k slots after Node 2. Thus, *the starting points of the backoff counters are misaligned by k slots*. **Right Panel: A success**. Node 1 starts a transmission at time 0. Node 2 hears this transmission after a propagation delay of m slots, and freezes its backoff. Receiver 1 receives the end of Node 1's transmission after a propagation delay of m_r slots, i.e., at time $T+m_r$, and starts sending an ACK. Since the propagation delays from Receiver 1 to both the nodes are equal, namely, m_r slots, both Nodes 1 and 2 hear the ACK from Receiver 1 at the same time, and hence, start their DIFS together, following which, they start their next backoffs together. Thus, no misalignment in the next backoff initiation happens in this case.

is that the node that initiates transmission earlier is the one that will have a delayed backoff in the next cycle, because it will hear the end of the other transmission later.

4. Observe that in the above argument, *the property of equal propagation delays among all transmitters is used crucially*. If the propagation delays were unequal, the backoff counters of all the nodes could be potentially misaligned with respect to one another (unlike the argument in Item 3 above, where all except one node start their backoffs together), and we would have to keep track of pairwise misalignments among the nodes, instead of a single misalignment, making the state space much larger (see also Sections VI and VII). *Hence, direct extension of the techniques in this paper to the case of unequal propagation delays will lead to a very complex state-space*.

5. Due to this misalignment of the backoff counters *we cannot apply the analytical approach in [1] and [2] in this case*, since there the authors were able to model the process evolution by focusing *only* on back-off times (see also Section V-B).

6. Such misalignment of backoff counters was also observed (even with zero propagation delay) and studied in the context of IEEE 802.11e EDCA; see [3], [8] and references therein. However, *a crucial difference compared to our setting is that the misalignment there is deterministic for given protocol parameters, whereas in the current setting, the misalignment is random*; this prevents the use of the techniques proposed in the EDCA context to address the current problem. □

B. A Detailed Markov Renewal Model

An *"activity"* in the medium is defined as the duration from the instant when a transmission starts in the medium, to the instant when some node is ready to start its next DIFS. For example, in the Left panel of Figure 6, there is an activity in the medium during the interval $[0, T+m]$, and in the Right panel of Figure 6, there is an activity in the medium during the interval $[0, T+m_r+ACK+m_r]$.

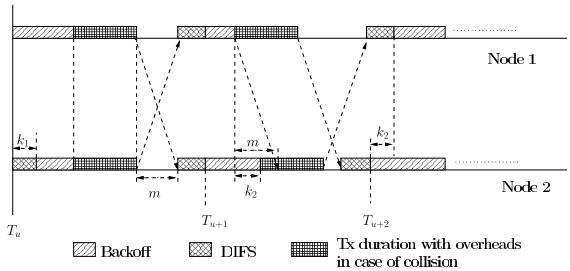

Fig. 7. **Transmission Cycles** for $n = 2$. The evolution of the timelines can be explained as follows. Node 1 happens to be the first to start its backoff after an activity in the medium. Node 2 starts its backoff after a misalignment of k_1 slots. Both the nodes happen to finish their backoffs together, and start a transmission at the same time, leading to a collision. In this case, the ends of their transmissions are aligned, and hence both the nodes sense the channel idle (after a propagation delay of m slots), and start their DIFS at the same time, following which they start fresh backoffs, with the starts of the backoff counters aligned. This time, Node 1 finishes its backoff first, and starts a transmission. Node 2 finishes its backoff k_2 slots after Node 1, where $k_2 < m$, thus leading to a collision, and subsequent misalignment of the starts of their next backoffs by k_2 slots, in the same manner as explained in the left panel of Figure 6, with Node 2 leading Node 1 by k_2 slots. Denote by T_u, the first instant after the u^{th} activity in the medium when some node starts counting down its backoff. The intervals $[T_u, T_{u+1}]$ and $[T_{u+1}, T_{u+2}]$ are, respectively, the $(u+1)^{th}$ and $(u+2)^{th}$ *transmission cycles*.

Let T_u be the first instant after the u^{th} activity in the medium when some node starts counting down its backoff. See, for example, Figure 7, which depicts a sample path of the system evolution for $n = 2$. We call the interval $[T_u, T_{u+1}]$ the $(u+1)^{th}$ *transmission cycle*. In each transmission cycle, there is exactly one activity in the medium.

Let $B_{u,i}, S_{u,i}, Z_{u,i}$, denote respectively the residual backoff count, backoff stage, and misalignment (w.r.t. T_u) of the start of backoff counter of Node i, $i = 1, 2, \ldots, n$ at T_u. Recalling the notation for the protocol parameters of IEEE 802.11 DCF, $S_{u,i} \in \{0, 1, \ldots, K\}$, $B_{u,i} \in \{1, \ldots, W_{S_{u,i}}\}$, and $Z_{u,i} \in \{0, 1, \ldots, m\}$. Then, the process $(\{B_{u,i}, S_{u,i}, Z_{u,i}\}_{i=1}^{n}, T_u)$ is a Markov Renewal Process [18], with $\{B_{u,i}, S_{u,i}, Z_{u,i}\}_{i=1}^{n}$ being the embedded Markov chain, whose transition structure is explained next.

Note that $(T_u + B_{u,i} + Z_{u,i})$ is the instant when Node i is scheduled to finish its backoff, and attempt a transmission in the $(u+1)^{th}$ transmission cycle. Let $\underline{B}_u = \min_{1\le i\le n}(B_{u,i} + Z_{u,i})$, and $I_u = \arg\min_{1\le i\le n}(B_{u,i} + Z_{u,i})$.

Observations:

1. $(T_u + B_u)$ and I_u are, respectively, the attempt instant, and Node id of the first node to attempt transmission in the $(u+1)^{th}$ transmission cycle.

2. A successful transmission happens *iff* for all $i \neq I_u$, $B_{u,i} + Z_{u,i} > \underline{B}_u + m$, and a collision happens otherwise. We need to consider only the integer part of the propagation delay between the transmitters in slots, i.e., m, since the probabilities of the events corresponding to success and collision are unaffected by the fractional part of the propagation delay; to see this, note that $B_{u,i}$ and $Z_{u,i}$ always take values in integer multiples of slots.

With the above information, the transition structure of the embedded Markov chain can be obtained without much difficulty; we provide the details in the Supplementary Material.

Remarks:

1. *For the zero-propagation-delay case, the Markov renewal model embedded at the epochs T_u is equivalent to the exact DTMC model (Section III) embedded at the backoff slot boundaries* in the following sense: for any given system, suppose we simulate the two models starting with the same initial conditions (backoff stages of the nodes), and the same random seed; the same random seed ensures that the backoff sampled by a Node i after the k^{th} retransmission of its j^{th} packet is the same for both the simulations, for all i, j, k. Then, the two models give rise to the same sample path for the system evolution (after reconstructing the original process in unconditional time from the backoff process obtained from the DTMC model). Since the DTMC model is known to give excellent accuracy [3], this establishes the accuracy of the Markov Renewal model for the zero propagation delay case.

2. We have simulated this detailed model for the case of $n = 2$, default backoff parameters of IEEE 802.11b, and a wide range of propagation delays (with $m = m_r$) to obtain the long run average collision probability, γ, and compared these analysis results against simulation results obtained from Qualnet.[5] The results are shown in Figure 8; it can be seen that the proposed model captures the system behavior very accurately for long run average collision probability. Similar observation holds for the long run average system throughput. □

However, the proposed model involves an embedded $3n$-dimensional Markov chain, whose state space has size $(nm + 1)(W_0 + W_1 + \cdots + W_K)^n$, where K is the retransmission limit for the protocol, and W_j is the contention window size for backoff stage j. For the default protocol parameters of IEEE 802.11b, the size of the state space is prohibitively large even for $m = 1$, and $n = 2$, making an exact analysis of the embedded Markov chain computationally intractable.

[5]after correcting an error in the default Qualnet implementation wherein an extra delay of m_r gets added to the NAV of the frozen node in addition to the correct value of $2m_r$.

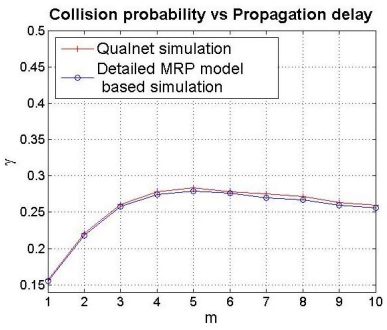

Fig. 8. Collision probability (γ) vs. propagation delay (m). Comparison of collision probabilities obtained via a Monte-Carlo simulation of the detailed MRP model against those obtained from Qualnet simulations [11].

We, therefore, focus on developing an approximate, parsimonious analysis.

Note, however, that we will use the detailed MRP model as a prototype of the actual system, and it will be simulations of this MRP model against which to check the accuracy of our approximate analysis technique. This approach is analogous to the exact Markov model in [2] being approximated by the decoupling approximation. The reasons for this choice are as follows: there is a distinct advantage of using a Monte Carlo simulation of this detailed model over using Qualnet (or any other event-driven) simulation for predicting the system performance. Qualnet simulation runs over backoff slots, and works by simulating all the details of the protocol at every node; on the other hand, the model-based simulator runs over transmission cycles, and eliminates all unnecessary details of the protocol. Hence, the model-based simulator can run much faster while achieving comparable accuracy (within 1-2% of Qualnet). Furthermore, it is easier to examine certain finer details of the system evolution using this model, which would otherwise be hard to do with Qualnet; for example, the conditional attempt rates introduced in Section VII can be easily obtained from a Monte-Carlo simulation of the above model, but hard to obtain from Qualnet.

VII. State Dependent Bernoulli Attempts (SDBA) Approximation of the Detailed Markov Renewal Model in Section VI

The analysis in [1] and [2] is based on a simple model of constant attempt rates, and can be viewed as an approximation to the detailed $2n$-dimensional Markov chain that represents the system without propagation delay. In this section, we introduce state-dependent attempt rates to develop an approximation to the Markov renewal model in Section VI-B. Our attempt is to introduce as few attempt rate parameters as possible.

A. State Dependent Attempt Rates

While retaining the embedded Markov process structure at the starts of transmission cycles, we aim to simplify the evolution of the process between these embedding points to reduce the computational complexity. In particular, we aim to avoid the exponential growth of the underlying state space size

with the number of nodes. The complexity of the analysis of the detailed process constructed in Section VI comes from the complex transition structure, due to the necessity to keep track of the various events, and their timing, between the embedding points.

One possible way to simplify the evolution between the embedding instants is to adopt the state independent, Bernoulli attempt process approximation in [1] and [2] (see Section III-A). Consider the consequence of this approximation on the success processes of the nodes. Observe that under this approximation, the probability that the next successful transmission in the system is due to a particular Node $j \in \{1, \ldots, n\}$ is $\frac{1}{n}$, *independent of which node made the last successful transmission*. To see this, note that under the constant, state independent attempt rate approximation, the evolution of the process from the last successful transmission onwards does not depend on the node id of the last successful node.

Let us compare this against observations from simulations. Revisiting Figure 2, we observe that the success process of the 600-node system (Panel 3) with the backoff parameters of Section IV-A is consistent with the conclusions drawn earlier from the state independent constant attempt rate approximation, but those conclusions clearly do not hold for the success process of the 20-node system (Panel 2) with the same backoff parameters, which exhibits significant correlation. Thus, the constant, state independent attempt rate approximation will not work in such cases.

Accounting for Short Term Unfairness in the Node Attempt Process*:* Taking cue from this, we adopt the Bernoulli attempt process approximation for the nodes as in[1] and [2], but introduce *state dependent attempt rates, namely, β_s, β_c, and β_d to distinguish among three cases: whether a node encountered a success, a collision, or an interruption (of its backoff; due to transmission by some other nodes), respectively, in the previous transmission cycle*. The rationale behind such choices of attempt rates is explained in the remarks at the end of this subsection. From our experience with such models, this also seems to be the model with the fewest additional parameters that works.

Observe that under this approximation, in order to construct the system evolution in a transmission cycle, we need to know the attempt rates of the nodes at the start of the transmission cycle, which, in turn, depend on the number of nodes that attempted in the last cycle, since the nodes that did not attempt (i.e., were interrupted) will attempt at rate β_d in the next cycle, while the nodes that attempted in the last cycle will attempt at rate β_s or β_c, depending on whether the last transmission was a success or a collision. Hence, we associate with each epoch T_u, a state, N_u, *the number of nodes that attempted in the previous cycle*. In the detailed model of Section VI, we did not need this state since we kept track of more detailed states, namely, the backoff stage, and the residual backoff of each node, which completely determine the subsequent evolution (including the number of nodes attempting in a transmission cycle).

Accounting for Possible Misalignment *in Case of Large Propagation Delay:* We saw in Section V-B that if we do not account for the *possible misalignment* of backoff counters of the nodes after a collision (Section VI-A), the resulting analysis is not accurate. To account for this, we associate with each T_u, another state, namely, the *misalignment*, Z_u, of the backoff counters of the nodes at T_u. Note that $Z_u = 0$ if there was a success in the last transmission cycle, and $Z_u = Z_{u,+} \in \{0, 1, \ldots, m\}$ otherwise. For example, in Figure 7, the *misalignments* at T_u, T_{u+1} and T_{u+2} are respectively k_1, 0, and k_2 slots.

Further note that to use the state dependent attempt rates, we need to know whether a transmission cycle ended in a success, or a collision. Observe that while $Z_u > 0$ clearly indicates a collision in the previous transmission cycle, $Z_u = 0$ could indicate either a collision or a success in the previous transmission cycle. To distinguish between these two cases, we introduce two new states, namely 0_s, and 0_c, indicating that there is no misalignment of the backoff counters at T_u, and that the previous transmission cycle ended in a success, or a collision respectively. Thus, in our new model, $Z_u \in \{0_s, 0_c, 1, \ldots, m\}$. Finally, note that $N_u = 1$ if $Z_u = 0_s$, and $N_u \geq 2$ otherwise.

The approximate model can be summarized as follows:

(A1) If $Z_u = 0_s$, all the nodes start their backoffs from T_u. The node that was successful in the previous transmission cycle attempts independently with probability β_s in each slot, conditioned on being in backoff. The other nodes attempt independently with probability β_d in each slot, conditioned on being in backoff. □

(A2) If $Z_u = 0_c$, all nodes start their backoffs from T_u. N_u of the nodes attempt independently with probability β_c in each slot, while the remaining $n - N_u$ nodes attempt independently with probability β_d in each slot, all conditioned on being in backoff. If $Z_u = k > 0$, N_u of the nodes attempt independently with probability β_c in each slot, conditioned on being in backoff, one starting from T_u, and the others, starting from $T_u + k$ (Remark 3, Section VI-A); the remaining $n - N_u$ nodes attempt independently with probability β_d in each slot, conditioned on being in backoff, starting from $T_u + k$. □

Remarks:

1) After a successful transmission in the system, we may expect the residual backoffs of the interrupted nodes to be relatively large compared to the next backoff of the successful node (which samples its backoff from the smallest contention window), especially for backoff sequences that lead to short term unfairness; thus, the attempt rates of the interrupted nodes can be expected to be significantly lower than that of the successful node. This is the rationale behind introducing the attempt rates β_s and β_d to distinguish between the successful node, and the interrupted nodes.

2) Following a similar rationale, in case of a collision, we may expect the nodes that were interrupted (did not participate in the collision) to have relatively large residual backoffs compared to the nodes involved in the collision. Also, since after a collision, a node will sample backoff from a larger contention window, its attempt rate after a collision can be expected to be lower than that after a success. Hence we introduce the attempt rate β_c to distinguish the colliding nodes from the interrupted nodes, as well as the successful node. □

The State Dependent Bernoulli Attempts Markov Renewal Process (SDBA MRP) Approximation: With these approximations, observe that the process $\{(Z_u, N_u), T_u\}$, is a Markov renewal process, the state space of the embedded Markov chain being $\{0_s, 0_c, 1, \ldots, m\} \times \{1, \ldots, n\}$. Also, observe that for $n = 2$ and arbitrary m, it suffices to consider only the state Z_u, thus reducing the state space. Similarly, for $m = 0$ and arbitrary n, it suffices to consider only the state N_u. We develop the details for these two cases. The underlying principles apply to the more general setting as well, but the equations become more involved.

B. Zero Propagation Delay, Arbitrary n: Analysis of the SDBA MRP for $m = 0$ and Arbitrary n, Given β_c, β_d, and β_s

The SDBA MRP model has n as a parameter, and requires the quantities β_c, β_d, and β_s, which are not known a priori. We shall explain how to compute β_c, β_d, and β_s in Sections VII-D, VII-E and VII-F. Given β_c, β_d, and β_s, let P be the transition probability matrix of the embedded Markov chain. We now proceed to write down the transition probabilities. We use the shorthand $p(n_a, n'_a)$ to denote the probability $Pr[N_{u+1} = n'_a | N_u = n_a]$.

Computation of $p(n_a, n'_a)$:

Define the sets $F(n_a, n'_a) = \{(i, j) : 0 \leq i \leq n_a, 0 \leq j \leq n - n_a, i + j = n'_a\}$ for all $n_a, n'_a \in \{1, \ldots, n\}$. Also define

$$q(n_a, n'_a) = \sum_{(i,j) \in F(n_a, n'_a)} \binom{n_a}{i} \binom{n - n_a}{j} \beta_x^i (1 - \beta_x)^{n_a - i} \times \beta_d^j (1 - \beta_d)^{n - n_a - j} \quad (3)$$

where $\beta_x = \beta_s$ if $n_a = 1$, and $\beta_x = \beta_c$, if $n_a > 1$.

Observe that given the information that n_a nodes are attempting at rate β_x, and remaining $(n - n_a)$ nodes are attempting at rate β_d, $q(n_a, n'_a)$ is the probability that n'_a nodes attempt together in a backoff slot, while the remaining $(n - n'_a)$ nodes remain silent.

Then we can write

$$p(n_a, n'_a) = (1 - \beta_x)^{n_a} (1 - \beta_d)^{n - n_a} p(n_a, n'_a) + q(n_a, n'_a) \quad (4)$$

Here, the first term corresponds to the event that none of the nodes attempt in the first backoff slot; in this case, due to the assumption of Bernoulli attempt processes, the system encounters a renewal with state n_a, and the conditional probability (given that none of the nodes attempted in the first slot) of the next state being n'_a remains $p(n_a, n'_a)$. Thus we have

$$p(n_a, n'_a) = \frac{q(n_a, n'_a)}{1 - (1 - \beta_x)^{n_a} (1 - \beta_d)^{n - n_a}} \quad (5)$$

where $\beta_x = \beta_s$ if $n_a = 1$, and $\beta_x = \beta_c$, if $n_a > 1$.

From the above transition probability structure, it is easy to observe that for positive attempt rates, the embedded DTMC is finite, irreducible, and hence, *positive recurrent*. Let π denote the stationary distribution of this DTMC, which can be obtained as the unique solution to the system of equations $\pi = \pi P$, subject to $\sum_{n_a \in \{1,2,\ldots,n\}} \pi(n_a) = 1$.

1) Obtaining the Collision Probability, γ: By symmetry, the long run average collision probability for all the nodes is the same, which we denote by γ. It is defined as

$$\gamma = \lim_{t \to \infty} \frac{C_i(t)}{A_i(t)}, \quad i = 1, 2, \ldots, n$$

where, $C_i(t)$ and $A_i(t)$ denote respectively, the number of collisions and the number of attempts by Node i until time t. Denoting $C(t) \stackrel{\triangle}{=} \sum_{i=1}^n C_i(t)$, the total number of collisions in the system until time t, and $A(t) \stackrel{\triangle}{=} \sum_{i=1}^n A_i(t)$, the total number of attempts in the system until time t, it is also easy to observe (by noting that the long run time-average collision rates, and the long run time-average attempt rates of all the nodes are equal by symmetry) that

$$\gamma = \lim_{t \to \infty} \frac{C(t)}{A(t)}$$

Denote by $\mathcal{C}$ and $\mathcal{A}$, respectively, the random variables representing the number of collisions, and the number of attempts in the system in a transmission cycle. Then, using Markov regenerative theory (see, for example, [18]), we have

$$\gamma = \frac{\sum_{n_a=1}^n \pi(n_a) E\mathcal{C}(n_a)}{\sum_{n_a=1}^n \pi(n_a) E\mathcal{A}(n_a)} \quad a.s \quad (6)$$

where, $E\mathcal{C}(n_a)$ and $E\mathcal{A}(n_a)$ denote respectively, the expected number of collisions, and attempts in the system in a transmission cycle starting with state n_a, and can be computed by using renewal arguments similar to those used for obtaining the transition probabilities earlier, and observing that every collision event involving n'_a nodes results in n'_a collisions (and involves n'_a attempts, one from each node), and every success event involves 1 attempt (from the successful node). We have, for all $n_a = 1, 2, \ldots, n$,

$$E\mathcal{C}(n_a) = \sum_{n'_a=2}^n p(n_a, n'_a) n'_a \quad (7)$$

$$E\mathcal{A}(n_a) = \sum_{n'_a=1}^n p(n_a, n'_a) n'_a \quad (8)$$

where, $\beta_x = \beta_s$ if $n_a = 1$, and $\beta_x = \beta_c$, if $n_a > 1$.

2) Obtaining the Normalized System Throughput, Θ: The normalized system throughput is defined as

$$\Theta = \lim_{t \to \infty} \frac{T(t)}{t}$$

where $T(t)$ is the total successful data transmission duration without overheads until time t.

Denote by $\mathcal{T}$, the random variable representing the duration of successful data transmission excluding overheads in a transmission cycle. Then, by Markov regenerative theory, we have

$$\Theta = \frac{\sum_{n_a=1}^n \pi(n_a) E\mathcal{T}(n_a)}{\sum_{n_a=1}^n \pi(n_a) EX(n_a)} \quad a.s \quad (9)$$

where, $E\mathcal{T}(n_a)$ and $EX(n_a)$ are, respectively, the mean duration of successful data transmission excluding overheads,

and the mean duration of the transmission cycle when the transmission cycle starts in state n_a. We can write down the expressions for $E\mathcal{T}(\cdot)$ and $EX(\cdot)$ using renewal arguments similar to those given earlier as follows.

$$E\mathcal{T}(n_a) = \frac{q(n_a,1)T_d}{1-(1-\beta_x)^{n_a}(1-\beta_d)^{n-n_a}} \tag{10}$$

$$EX(n_a) = \frac{1+q(n_a,1)T_s+\sum_{n'_a=2}^{n} q(n_a,n'_a)T_c}{1-(1-\beta_x)^{n_a}(1-\beta_d)^{n-n_a}} \tag{11}$$

for all $n_a = 1,\ldots,n$. As before, $\beta_x = \beta_s$ if $n_a = 1$, and $\beta_x = \beta_c$, if $n_a > 1$. Also, T_s is the time duration in a successful transmission cycle from the start of the data transmission in the medium until the time the medium is idle again, and the nodes start counting their backoffs (i.e., until the start of the next transmission cycle), and is given by

$$T_s = T_d + ACK + 2\times PHY\ HDR + 2T_o + SIFS + DIFS$$

and T_c is the time duration in a collision transmission cycle from the start of the first data transmission in the medium until the time the nodes start counting their backoffs (i.e., until the start of the next transmission cycle), and is given by

$$T_c = T_d + PHY\ HDR + T_o + SIFS + DIFS$$

In the above expressions, T_o denotes the Rx-to-Tx turnaround time.

This completes the analysis of the system evolution for $m = 0$ and arbitrary n, given β_s, β_d, β_c.

A Generalization of the Analysis in [1]:

Until this point, what has been shown is the procedure to get the performance measures if the attempt rates, $\beta_s, \beta_c, \beta_d$ are given. It is an interesting exercise to relate this to what was done in the well known analysis in [1] (Section III-A). Indeed, if we set $\beta_s = \beta_c = \beta_d = \beta$, i.e., a state independent, constant attempt rate, we get back from Equation 6, the collision probability as $\gamma = 1-(1-\beta)^{n-1}$, i.e., the same expression as in the analysis in [1] (Equation 2); details are in the Supplementary Material. Thus, our analysis can indeed be viewed as a generalization of the analysis in [1] with *state dependent* attempt rates. □

C. Arbitrary Propagation Delay, and $n = 2$: Analysis of the SDBA MRP for $n = 2$ and Arbitrary m, Given β_c, β_d, and β_s

For $n = 2$ and arbitrary m, $\{Z_u, T_u\}$ is a Markov renewal process (MRP), the state space of the embedded Markov chain being $\{0_s, 0_c, 1, \ldots, m\}$. This Markov renewal process model has m as a parameter, and requires the quantities β_c, β_d, and β_s, which are not known a priori. We shall explain how to compute β_c, β_d, and β_s in Section VII-D. Given β_c, β_d, and β_s, let P be the transition probability matrix of the embedded Markov chain. Using the assumption of Bernoulli attempt processes of the nodes, along with observations from Section VI, one can obtain P; we provide the details in the Supplementary Material. It turns out that for positive attempt rates, the Markov chain is positive recurrent; denote by π, its unique stationary distribution.

1) Obtaining the Collision Probability, γ, for $n = 2$, and Arbitrary m: By symmetry, the long run average collision probability for both the nodes is the same, which we denote by γ. As in the previous case, denoting $C(t) \stackrel{\triangle}{=} \sum_{i=1}^{2} C_i(t)$, the total number of collisions in the system until time t, and $A(t) \stackrel{\triangle}{=} \sum_{i=1}^{2} A_i(t)$, the total number of attempts in the system until time t, we have

$$\gamma = \lim_{t\to\infty} \frac{C(t)}{A(t)}$$

Denote by $\mathcal{C}$ and $\mathcal{A}$, respectively, the random variables representing the number of collisions, and the number of attempts in the system in a transmission cycle. Then, using Markov regenerative theory, we have

$$\gamma = \frac{\sum_{k\in\{0_s,0_c,\ldots,m\}} \pi(k) E\mathcal{C}(k)}{\sum_{k\in\{0_s,0_c,\ldots,m\}} \pi(k) E\mathcal{A}(k)} \quad a.s \tag{12}$$

where, $E\mathcal{C}(k)$ and $E\mathcal{A}(k)$ denote respectively, the expected number of collisions, and attempts in the system in a transmission cycle starting with state k, and can be computed by using certain renewal arguments similar to those used for obtaining the transition probability matrix P (see the Supplementary Material), and observing that every collision event results in 2 collisions (and involves 2 attempts, one from each node), and every success event involves 1 attempt (from the successful node). We write down the expressions for $E\mathcal{C}(\cdot)$ and $E\mathcal{A}(\cdot)$ below.

$$E\mathcal{C}(0_s) = \frac{\beta_s(1-\beta_d)q_d\cdot 2 + \beta_d(1-\beta_s)q_s\cdot 2 + 2\beta_s\beta_d}{1-(1-\beta_s)(1-\beta_d)} \tag{13}$$

$$E\mathcal{A}(0_s) = \frac{\beta_s(1-\beta_d)(1+q_d)+\beta_d(1-\beta_s)(1+q_s)+2\beta_s\beta_d}{1-(1-\beta_s)(1-\beta_d)} \tag{14}$$

$$E\mathcal{C}(0_c) = \frac{2\beta_c(1-\beta_c)q_c\cdot 2 + 2\beta_c^2}{1-(1-\beta_c)^2} \tag{15}$$

$$E\mathcal{A}(0_c) = \frac{2\beta_c(1-\beta_c)(1+q_c)+2\beta_c^2}{1-(1-\beta_c)^2} \tag{16}$$

$$E\mathcal{C}(k) = (1-\beta_c)^k E\mathcal{C}(0_c) + \sum_{j=1}^{k}(1-\beta_c)^{(j-1)}\beta_c p_j^{(k)}\cdot 2 \quad \forall k = 1,\ldots,m \tag{17}$$

$$E\mathcal{A}(k) = (1-\beta_c)^k E\mathcal{A}(0_c) + \sum_{j=1}^{k}(1-\beta_c)^{(j-1)}\beta_c(1+p_j^{(k)}) \quad \forall k = 1,\ldots,m \tag{18}$$

where, we define $q_d \stackrel{\triangle}{=} 1-(1-\beta_d)^m$, $q_s \stackrel{\triangle}{=} 1-(1-\beta_s)^m$, and $q_c \stackrel{\triangle}{=} 1-(1-\beta_c)^m$. This completes the computation of the average collision probability, γ, given the conditional attempt rates β_d, β_s, β_c.

2) Obtaining the Normalized System Throughput, Θ, for $n = 2$, and Arbitrary m: The normalized system throughput is defined as

$$\Theta = \lim_{t\to\infty} \frac{T(t)}{t}$$

where $T(t)$ is the total successful data transmission duration without overheads until time t.

Denote by $\mathcal{T}$, the random variable representing the duration of successful data transmission excluding overheads in a transmission cycle. Then, by Markov regenerative theory, we have

$$\Theta = \frac{\sum_{k\in\{0_s,0_c,\ldots,m\}} \pi(k) E\mathcal{T}(k)}{\sum_{k\in\{0_s,0_c,\ldots,m\}} \pi(k) EX(k)} \quad a.s \tag{19}$$

where, $E\mathcal{T}(k)$ and $EX(k)$ are, respectively, the mean duration of successful data transmission excluding overheads, and the mean duration of the transmission cycle when the transmission cycle starts in state k. Letting T_d, T_o, and Δ denote respectively the data packet duration, Rx-to-tx turnaround time, and propagation delay, we can write down the expressions for $E\mathcal{T}(\cdot)$ and $EX(\cdot)$ using certain renewal arguments as follows.

$$\begin{aligned} EX(0_s) = {} & \frac{1}{1-(1-\beta_s)(1-\beta_d)}[1+(\beta_s\beta_d+\beta_s(1-\beta_d)q_d \\ & +\beta_d(1-\beta_s)q_s)T_c+(\beta_s(1-\beta_d)(1-q_d) \\ & +\beta_d(1-\beta_s)(1-q_s))T_s] \end{aligned} \tag{20}$$

$$E\mathcal{T}(0_s) = \frac{(\beta_s(1-\beta_d)(1-q_d)+\beta_d(1-\beta_s)(1-q_s))T_d}{1-(1-\beta_s)(1-\beta_d)} \tag{21}$$

$$\begin{aligned} EX(0_c) = {} & \frac{1}{1-(1-\beta_c)^2}[1+(\beta_c^2+2\beta_c(1-\beta_c)q_c)T_c \\ & +2\beta_c(1-\beta_c)(1-q_c)T_s] \end{aligned} \tag{22}$$

$$E\mathcal{T}(0_c) = \frac{2\beta_c(1-\beta_c)(1-q_c)T_d}{1-(1-\beta_c)^2} \tag{23}$$

$$\begin{aligned} EX(k) = {} & (1-\beta_c)^k(k+EX(0_c))+\sum_{j=1}^{k}(1-\beta_c)^{j-1}\beta_c[j \\ & +(1-p_j^{(k)})T_s+p_j^{(k)}T_c] \quad \forall k\in\{1,\ldots,m\} \end{aligned} \tag{24}$$

$$E\mathcal{T}(k) = (1-\beta_c)^k E\mathcal{T}(0_c)+\sum_{j=1}^{k}(1-\beta_c)^{j-1}\beta_c(1-p_j^{(k)})T_d \tag{25}$$

where, T_s is the time duration in a successful transmission cycle from the start of the data transmission in the medium until the time the medium is idle again, and some node starts counting its backoff (i.e., until the start of the next transmission cycle), and is given by

$$\begin{aligned} T_s = {} & T_d + ACK + 2\times PHY\ HDR + 2T_o + SIFS \\ & + DIFS + 2\Delta_r \end{aligned}$$

and T_c is the time duration in a collision transmission cycle from the start of the first data transmission in the medium until the time some node starts counting its backoff (i.e., until the start of the next transmission cycle), and is given by

$$T_c = T_d + PHY\ HDR + T_o + SIFS + DIFS + \Delta$$

This completes the analysis of the system evolution for $n = 2$ and arbitrary m, given β_s, β_d, β_c.

It remains to obtain the state dependent attempt rates β_s, β_d, β_c for both the cases, namely, (i) $m = 0$ and arbitrary n, and (ii) arbitrary m and $n = 2$. To do this, we shall set up a system of fixed point equations in β_c, β_d, and β_s by modeling the evolution at a tagged node. This can, in turn, be solved iteratively to yield the rates.

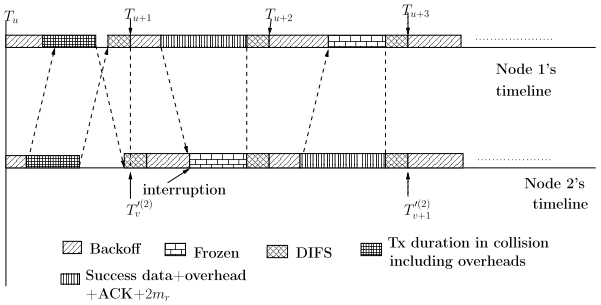

Fig. 9. **Backoff Cycles** for a tagged node, Node 2 in this case. The two timelines demonstrate the system evolution over three consecutive transmission cycles, with T_u,..., T_{u+3} being the start and end points of the transmission cycles. The explanation of the evolution of these timelines is similar to those in Figures 6 and 7. Denote by $T_v'^{(i)}$, *the start of the transmission cycle following the* v^{th} *transmission by the tagged node,* i, Node 2 in this example. The interval $[T_v'^{(2)}, T_{v+1}'^{(2)}]$ is called a *backoff cycle* of Node 2, since in this interval, Node 2 completes one full backoff. Note that the tagged node can have *exactly one attempt (backoff completion)*, and several intermediate backoff *interruptions* in a backoff cycle. During each system transmission cycle $[T_u, T_{u+1}]$, any node can have at most one backoff segment. Thus the backoff chosen at the start of a tagged node's backoff cycle is partitioned into several backoff segments over a random number of system transmission cycles during the tagged node's backoff cycle. Thus, a backoff cycle can encompass several transmission cycles during which the tagged node was interrupted (i.e., did not attempt).

D. Obtaining the State Dependent Attempt Rates: a Fixed Point Approach

In Sections VII-B and VII-C, we assumed Bernoulli attempt processes with state dependent rates for *all* nodes in modeling the system evolution (to obtain the performance measures, given the attempt rates). We next show how to determine the state dependent attempt rates. Analogous to the approach in [2], we consider a tagged node whose successive backoffs are sampled from uniform distributions with the given backoff parameters, whereas the other nodes attempt in Bernoulli processes with state dependent rates. With this model, we aim to determine the attempt rate of the tagged node in each of the states. This results in a system of fixed point equations, akin to the modeling in [1] and [2].

Let the tagged node be Node i, and identify embedding instants $T_v'^{(i)}$ in this process as explained in Figure 9, where the transmission cycle break-points $T_u, \ldots$ are shown, along with the epochs $T_v'^{(2)} \ldots$ for Node 2 (the tagged node). After each such epoch, the tagged node samples a new backoff, using its current backoff stage S_v. We associate with each $T_v'^{(i)}$, three states: (i) $S_v \in \{0, 1, \ldots, K\}$, Node $i's$ new backoff stage, (ii) $X_v \in \{0_s, 0_c, \pm 1, \ldots, \pm m\}$, Node $i's$ *relative* misalignment w.r.t the other nodes at $T_v'^{(i)}$, where $X_v = +k$ means Node i will start backoff at $T_v'^{(i)} + k$, and $X_v = -k$ means Node i starts backoff at $T_v'^{(i)}$, while all the others start at $T_v'^{(i)} + k$. Observe that $S_v > 0 \Rightarrow X_v \neq 0_s$, since a successful transmission by Node i would have reset S_v to zero. (iii) $N_v \in \{1, \ldots, n\}$, number of nodes (including the tagged

Node i) that attempted in the just concluded *transmission cycle*.

For $n = 2$ and arbitrary m, N_v is completely determined by X_v (e.g., $X_v = 0_s \Rightarrow N_v = 1$), thus reducing the state space. On the other hand, for $m = 0$ and arbitrary n, X_v is completely determined by N_v (e.g., $N_v > 1 \Rightarrow X_v = 0_c$), thus again reducing the state space.

Notice from Figure 9 that *transmission cycles* are common to the entire system, whereas *backoff cycles* are defined for each node. Each backoff cycle of a node *comprises one or more transmission cycles of the system. The backoff cycle of a tagged node can comprise several successful transmissions and/or collisions by the other nodes*, and ends at the end of a transmission cycle in which the tagged node transmits.

Continuing the earlier list of approximation steps in our analysis approach, we have:

(A3) Node i samples its successive back-offs from a uniform distribution, as in the standard. When a new backoff cycle starts for Node i, if $X_v = 0_s$, the other nodes, conditioned on being in backoff, attempt independently in each slot with probability β_d *until the end of the first transmission cycle within this backoff cycle*. If $X_v \neq 0_s$, $N_v - 1$ of the nodes, conditioned on being in backoff, attempt independently in each slot with probability β_c, and the remaining $n - N_v$ nodes, conditioned on being in backoff, attempt independently in each slot with probability β_d *until the end of the first transmission cycle within this backoff cycle*. □

(A4) If Node i is interrupted within a backoff cycle due to attempts by n_a other nodes ($1 \leq n_a \leq n-1$), thus freezing its backoff (see Figure 9), then in the next transmission cycle within this backoff cycle, Node i resumes its residual backoff countdown, all the $n - 1 - n_a$ nodes (excluding Node i) that did not attempt in the previous transmission cycle attempt independently in each slot with probability β_d, conditioned on being in backoff, while the n_a nodes that attempted in the previous transmission cycle attempt with probability β_c or β_s (depending on whether the previous transmission cycle ended in collision or success, i.e., whether $n_a > 1$ or $n_a = 1$) in each slot, conditioned on being in backoff. □

In Sections VII-E and VII-F we show how to obtain the state dependent attempt rates of the tagged node. In order to emphasize the fixed point nature of the analysis, the state dependent rates of the tagged node are also denoted as β_d, β_s, and β_c.

E. Zero Propagation Delay ($m = 0$), Arbitrary n: Computation of the Attempt Rates for the SDBA MRP Approximation

Under assumptions (A3)-(A4), observe that for $m = 0$ and arbitrary n, the process $\{(S_v, N_v), T_v^{'(i)}\}$ is a Markov renewal process (MRP), with the state space of the embedded Markov chain being $\{0, \ldots, K\} \times \{1, \ldots, n\}$. This Markov renewal process has as its parameters the attempt rates of the nodes other than the tagged node, i.e., $\beta_s, \beta_d, and \beta_c$.

It can be shown that the embedded Markov chain has a unique stationary distribution, denoted by ψ. We provide the detailed derivation of this stationary distribution in the Supplementary Material. We discuss next, how we can compute the state dependent attempt rates of the tagged node, β_d, β_c and β_s, given ψ, and the attempt rates of the nodes other than the tagged node, i.e., β_d, β_c and β_s.

Recall that β_s and β_c are the mean attempt rates of a node in a transmission cycle after it resumes backoff following a successful transmission, and a collision, respectively, while β_d is the mean attempt rate of a node in a transmission cycle after it resumes backoff following an interruption. Thus, observe that in a backoff cycle of a tagged node, the contributions to β_s and β_c come from only the first transmission cycle within the backoff cycle, whereas the remainder (if any) of the backoff cycle contributes towards β_d.

1) Computation of β_d: Looking at the backoff evolution of the tagged Node i (see Figure 9), we can define β_d more formally as

$$\beta_d = \lim_{t\to\infty} \frac{\sum_{k=1}^{N(t)} \mathbf{1}_{\{\text{Node } i \text{ interrupted in backoff cycle } k\}}}{\sum_{k=1}^{N(t)} B_{r,k}}$$

where, $N(t)$ is the number of backoff cycles until time t, and $B_{r,k}$ is the *residual backoff* to be counted by Node i from the point of first interruption until its backoff completion in backoff cycle k provided that it was interrupted; $B_{r,k} = 0$ if Node i was not interrupted in backoff cycle k. It suffices to count the residual backoff from first interruption to backoff completion since the node does not sample any fresh backoff in between, and any intermediate interruption will find the node counting parts of the same residual backoff. Thus, the denominator is the total residual backoff counted by Node i until time t *after being interrupted*. The numerator is the total number of attempts made by Node i until time t upon completion of its residual backoff countdown after interruptions. Note that by our definition of backoff cycles, each backoff cycle must end with an attempt by Node i; the indicator function simply tracks whether the attempt followed an interruption or not.

Denote by $\mathcal{B}_r$, the random variable representing the residual backoff counted by Node i from the point of first interruption until its backoff completion in a backoff cycle. Then, by Markov Regenerative theory,

$$\beta_d = \frac{\sum_{(s,n_a)} \psi(s,n_a) P_I(s,n_a)}{\sum_{(s,n_a)} \psi(s,n_a) E\mathcal{B}_r(s,n_a)} \quad a.s \tag{26}$$

where, $P_I(s,n_a)$ is the probability that Node i is interrupted when the backoff completion cycle starts in state (s,n_a), and $E\mathcal{B}_r(s,n_a)$ is the mean residual backoff counted by Node i from its first interruption until its backoff completion in a backoff cycle that started with state (s,n_a); they can be computed as follows.

Computation of $P_I(\cdot,\cdot)$:

When the backoff cycle starts in state (s,n_a), we know from (A3) that during the first transmission cycle within this backoff cycle, $(n_a - 1)$ nodes will attempt w.p. β_c in each slot, and the remaining $(n - n_a)$ nodes (that did not attempt in the previous cycle) will attempt w.p. β_d in each slot. Suppose Node i samples a backoff of l slots uniformly from $[1, W_s]$. Then, Node i will be interrupted if at least one of the other nodes attempts within the first $(l-1)$ slots. This happens with

probability $1-((1-\beta_c)^{n_a-1}(1-\beta_d)^{n-n_a})^{l-1}$. Thus, we have

$$P_I(s,n_a)=\frac{1}{W_s}\sum_{l=1}^{W_s}\left[1-((1-\beta_c)^{n_a-1}(1-\beta_d)^{n-n_a})^{l-1}\right] \tag{27}$$

for all $s\in\{0,\ldots,K\}$, $n_a\in\{1,\ldots,n\}$.

Computation of $E\mathcal{B}_r(s,n_a)$:

Consider a backoff cycle starting with state (s,n_a). Suppose Node i samples (uniformly from $\{1,1,\ldots,W_s\}$) a backoff of l slots. As was explained earlier, to interrupt Node i, at least one other node must make an attempt by slot $l-1$. Suppose one or more of the other nodes make an attempt at slot w, $1\le w\le l-1$; this happens with probability $((1-\beta_c)^{n_a-1}(1-\beta_d)^{n-n_a})^{w-1}(1-(1-\beta_c)^{n_a-1}(1-\beta_d)^{n-n_a})$. In this case, the residual backoff of Node i is $(l-w)$. Thus, we have, for any $s\in\{0,\ldots,K\}$, and $n_a\in\{1,\ldots,n\}$,

$$\begin{aligned}E\mathcal{B}_r(s,n_a)=&\frac{1}{W_s}\sum_{l=1}^{W_s}\sum_{w=1}^{l-1}(l-w)\\&\times((1-\beta_c)^{n_a-1}(1-\beta_d)^{n-n_a})^{w-1}\\&\times(1-(1-\beta_c)^{n_a-1}(1-\beta_d)^{n-n_a})\end{aligned} \tag{28}$$

2) Computation of β_s: Looking at the backoff evolution of the tagged Node i, we can define β_s more formally as

$$\beta_s=\lim_{t\to\infty}\frac{\sum_{k=1}^{N_s(t)}\mathbf{1}_{\{\text{Node } i \text{ was not interrupted in backoff cycle } k\}}}{\sum_{k=1}^{N_s(t)}B_{s,k}}$$

where, $N_s(t)$ is the number of backoff cycles until time t that start with the state $(0,1)$ (implying that Node i was successful in the previous transmission cycle), and $B_{s,k}$ is the backoff counted by Node i *in the transmission cycle that started along with backoff cycle* k; in other words, $B_{s,k}$ is the backoff counted by Node i until it gets interrupted, or completes its backoff, whichever is earlier. Thus, the denominator is the total backoff counted by Node i until time t, in those transmission cycles that followed a successful transmission by Node i. Similarly, the numerator is the total number of attempts by Node i until time t in those transmission cycles that followed a successful transmission by Node i.

Denote by $\mathcal{B}_s$, the random variable representing the backoff counted by Node i in the first transmission cycle within a backoff cycle starting in state $(0,1)$. Then, by Markov regenerative theory, it follows that

$$\beta_s=\frac{1-P_I(0,1)}{E\mathcal{B}_s(0,1)}\quad a.s. \tag{29}$$

where, $E\mathcal{B}_s(0,1)$ is the mean time spent in backoff by Node i until it gets interrupted, or completes its backoff in the backoff cycle starting in state $(0,1)$, and can be computed as follows.

Suppose Node i samples (uniformly from $\{1,\ldots,W_0\}$) a backoff of l slots. To interrupt Node i, at least one of the other nodes must attempt within slot $(l-1)$. Now there are two possibilities:

1. None of the other nodes attempt up to slot $(l-1)$. Then Node i does not get interrupted, and its backoff count is l. This happens with probability $(1-\beta_d)^{(n-1)(l-1)}$.

2. One or more of the other nodes attempt at slot w, $1\le w\le l-1$. Then, Node i is interrupted, and its backoff counted until interruption is w. This happens with probability $(1-\beta_d)^{(n-1)(w-1)}(1-(1-\beta_d)^{n-1})$.

Combining all of these together,

$$\begin{aligned}E\mathcal{B}_s(0,1)=\frac{1}{W_0}\sum_{l=1}^{W_0}\Bigg[&(1-\beta_d)^{(n-1)(l-1)}l\\&+\sum_{w=1}^{l-1}w(1-\beta_d)^{(n-1)(w-1)}(1-(1-\beta_d)^{n-1})\Bigg]\end{aligned} \tag{30}$$

3) Computation of β_c: Looking at the backoff evolution of the tagged Node i, we can define β_c more formally as

$$\beta_c=\lim_{t\to\infty}\frac{\sum_{k=1}^{N_c(t)}\mathbf{1}_{\{\text{Node } i \text{ was not interrupted in backoff cycle } k\}}}{\sum_{k=1}^{N_c(t)}B_{c,k}}$$

where, $N_c(t)$ is the number of backoff cycles until time t that start with states other than $(0,1)$ (implying that Node i encountered a collision in the previous transmission cycle), and $B_{c,k}$ is defined as the backoff counted by Node i *in the transmission cycle that started along with backoff cycle* k; in other words, $B_{c,k}$ is the backoff counted by Node i until it gets interrupted, or completes its backoff, whichever is earlier. Thus, the denominator is the total backoff counted by Node i until time t, in those transmission cycles that followed a collision by Node i. Similarly, the numerator is the total number of attempts by Node i until time t in those transmission cycles that followed a collision by Node i.

Denote by $\mathcal{B}_c$, the random variable representing the backoff counted by Node i in the first transmission cycle following a collision involving Node i. Then, by Markov regenerative theory, it follows that

$$\beta_c=\frac{\sum_{(s,n_a)\neq(0,1)}\psi(s,n_a)(1-P_I(s,n_a))}{\sum_{(s,n_a)\neq(0,1)}\psi(s,n_a)E\mathcal{B}_c(s,n_a)}\quad a.s \tag{31}$$

where, $E\mathcal{B}_c(s,n_a)$ is the mean time spent in backoff by Node i until it gets interrupted, or completes its backoff in the backoff cycle starting in state (s,n_a), and can be computed as follows.

Suppose Node i samples (uniformly from $\{1,\ldots,W_s\}$) a backoff of l slots. As explained earlier, to interrupt Node i, at least one of the other nodes must make an attempt by slot $l-1$. Now, there are two possibilities:

1. None of the other nodes attempt up to slot $(l-1)$. Node i does not get interrupted, and its backoff count is l. This happens with probability $((1-\beta_c)^{n_a-1}(1-\beta_d)^{n-n_a})^{l-1}$.

2. One or more of the other nodes attempt at slot w, $1\le w\le (l-1)$. Then, Node i is interrupted, and its backoff count until interruption is w. This happens with probability $((1-\beta_c)^{n_a-1}(1-\beta_d)^{n-n_a})^{w-1}(1-(1-\beta_c)^{n_a-1}(1-\beta_d)^{n-n_a})$.

Combining these together, we have, for any $n_a \in \{2,\ldots,n\}$, and any $s \in \{0,\ldots,K\}$,

$$E\mathcal{B}_c(s,n_a) = \frac{1}{W_s}\sum_{l=1}^{W_s}\Big[l((1-\beta_c)^{n_a-1}(1-\beta_d)^{n-n_a})^{l-1} + \sum_{w=1}^{l-1} w((1-\beta_c)^{n_a-1}(1-\beta_d)^{n-n_a})^{w-1} \times (1-(1-\beta_c)^{n_a-1}(1-\beta_d)^{n-n_a})\Big] \quad (32)$$

4) A System of Fixed Point Equations: Equations 26-32 along with the expressions for the stationary probabilities $\psi(s,n_a)$ (derived in the Supplementary Material) form a system of vector fixed point equations in (β_d,β_c) (observe from Eqns. 27 and 30 that β_s is a deterministic function of β_d alone), which can be solved using an iterative procedure until convergence to obtain the attempt rates β_d, β_s, and β_c. For the case of $m = 0$ and arbitrary n, this completes the characterization of the SDBA MRP, that serves as our approximation to the detailed MRP in Section VI-B.

5) Computation of the Average Attempt Rate, β, Over All Backoff Time: The backoff cycle analysis can be used to obtain the long run average attempt rate, β, averaged over all backoff time (irrespective of system state). This is the quantity that was used in the fixed point approximation proposed in [1] and [2]; see Section III-A.

To obtain β, note that each backoff cycle contains exactly one attempt by the tagged node, and the backoff counted by the tagged node in the entire backoff cycle contributes towards β. In a backoff cycle starting in state (s,n_a), the mean backoff counted by the tagged node is clearly $(W_s+1)/2$. Thus, using Markov regenerative analysis, we have

$$\beta = \frac{1}{\sum_{(s,n_a)}\psi(s,n_a)\frac{W_s+1}{2}} \quad (33)$$

F. Arbitrary Propagation Delay m, $n = 2$: Computation of the Attempt Rates for the SDBA MRP Approximation

Under assumptions (A3)-(A4), observe that for $n = 2$ and arbitrary m, the process $\{(S_v,X_v),T_v'^{(i)}\}$ is a Markov Renewal process (MRP) with state space of the embedded Markov chain being $\{0,\ldots,K\}\times\{0_s,0_c,\pm1,\ldots,\pm m\}$.

1) Transition Structure of the Embedded Markov Chain for $n = 2$ and Arbitrary m: Let Q denote the transition probability matrix of the embedded DTMC at the epochs $T_v'^{(i)}$. We denote by W_s, the contention window size for backoff stage s, $s \in \{0,1,\ldots,K\}$. Denote the tagged node as Node i, and the only other node as Node j.

Let $Q_I[(s_2,x_2)|(s_1,x_1)]$ (respectively, $P_{nI}[(s_2,x_2)|(s_1,x_1)]$) be the probability that Node i is (respectively, is not) interrupted in a backoff cycle starting in state (s_1,x_1), *and* its backoff completion results in state (s_2,x_2).

Then, we can write, for any $s \in \{0,\ldots,K\}$, any $x \in \{0_s,0_c,\pm1,\ldots,\pm m\}$, and any $x' \in \{0_c,\pm1,\ldots,\pm m\}$,

$$Q((s,x),(0,0_s)) = P_{nI}[(0,0_s)|(s,x)] + Q_I[(0,0_s)|(s,x)] \quad (34)$$

$$Q((s,x),((s+1)mod(K+1),x')) = P_{nI}[((s+1)mod(K+1),x')|(s,x)] + Q_I[((s+1)mod(K+1),x')|(s,x)] \quad (35)$$

All other entries in Q are zero; since we embedded after transmissions of the tagged node, there are only two possibilities: success or collision of the tagged node's transmission.

Computation of the probabilities $Q_I[(\cdot,\cdot)|(\cdot,\cdot)]$, and $P_{nI}[(\cdot,\cdot)|(\cdot,\cdot)]$ involves certain renewal arguments, along with the assumption of Bernoulli attempt process at Node j, and the uniform backoff process of Node i; we leave the details to the Supplementary Material. It turns out that the Markov chain is *positive recurrent* for non-zero attempt rates. Denote by ψ, the unique stationary distribution of this Markov chain. We next proceed to obtain the mean attempt rates β_d, β_s, and β_c; the procedure is along the same lines as in Section VII-E.

2) Computation of β_d for $n = 2$, Arbitrary m: If the back-off cycle starts in the state (s,x), let $P_I(s,x)$ be the probability of the tagged node's back-off cycle being interrupted by a success of the other node. If such an interruption occurs, let $\mathcal{B}_r(s,x)$ be the residual back-off time of the tagged node (in this back-off cycle) after the interruption (note that $\mathcal{B}_r(s,x) = 0$ if an interruption does not occur). For example, in Figure 9, the backoff counted by Node 2 (tagged node) *after the interruption* until its backoff completion in the backoff cycle $[T_v',T_{v+1}']$ contributes towards β_d. With these observations, using Markov regenerative analysis, we have (see [16] for details).

$$\beta_d = \frac{\sum_{(s,x)}\psi(s,x)P_I(s,x)}{\sum_{(s,x)}\psi(s,x)E\mathcal{B}_r(s,x)} \quad a.s \quad (36)$$

For all $s \in \{0,1,\ldots,K\}$, and for all $x \in \{0_s,0_c,\pm1,\ldots,\pm m\}$,

$$P_I(s,x) = \frac{1}{W_s}\sum_{l=m-x+2}^{W_s}[1-(1-\beta_x)^{(l-(m-x+1))}] \quad (37)$$

$$E\mathcal{B}_r(s,x) = \frac{1}{W_s}\sum_{l=m-x+2}^{W_s}\sum_{w=1}^{l-(m-x+1)}(1-\beta_x)^{w-1} \times \beta_x(l-(w+m-x)) \quad (38)$$

with $\beta_x = \beta_d$ if $x = 0_s$, and $\beta_x = \beta_c$ otherwise.

3) Computation of β_s: The definition of β_s concerns only those transmission cycles immediately following a successful transmission by the tagged node, i.e., *the first transmission cycle within each backoff cycle (of the tagged node) starting in state* $(0,0_s)$. For example, in Figure 9, the transmission cycle starting at $T_{v+1}'^{(i)}$ will contribute towards β_s of Node 2 (the tagged node). Let $\mathcal{B}_s(0,0_s)$ denote the backoff counted by the tagged node in such a transmission cycle. If the tagged

node makes an attempt in this first transmission cycle (thus ending the backoff cycle *without getting interrupted*), then that attempt counts towards β_s. With these observations, we have (see [16]),

$$\beta_s = \frac{1 - P_I(0,0_s)}{E\mathcal{B}_s(0,0_s)} \quad a.s. \tag{39}$$

$$E\mathcal{B}_s(0,0_s) = \frac{1}{W_0}\frac{(m+1)(m+2)}{2} + \frac{1}{W_0}\sum_{l=m+2}^{W_0}[(1-\beta_d)^{(l-m-1)}l + \sum_{w=1}^{l-(m+1)}(1-\beta_d)^{w-1}\beta_d(w+m)] \tag{40}$$

4) Computation of β_c: The definition of β_c concerns only those transmission cycles immediately following a collision by the tagged node, i.e., *the first transmission cycle within each backoff cycle (of the tagged node) starting in state* $(s,x) \neq (0,0_s)$. For example, in Figure 9, the transmission cycle starting at $T_v'^{(i)}$ will contribute towards β_c of Node 2 (the tagged node). Let $\mathcal{B}_c(s,x)$ denote the backoff counted by the tagged node in such a transmission cycle. If the tagged node makes an attempt in this first transmission cycle (thus ending the backoff cycle *without getting interrupted*), then that attempt counts towards β_c. With these observations, we have (see [16]),

$$\beta_c = \frac{\sum_{(s,x)\neq(0,0_s)}\psi(s,x)(1-P_I(s,x))}{\sum_{(s,x)\neq(0,0_s)}\psi(s,x)E\mathcal{B}_c(s,x)} \quad a.s \tag{41}$$

For any $x \in \{0_s, 0_c, \pm 1, \ldots, \pm m\}$, and any $s \in \{0, \ldots, K\}$,

$$E\mathcal{B}_c(s,x) = \frac{1}{W_s}\sum_{l=1}^{m-x+1} l + \frac{1}{W_s}\sum_{l=m-x+2}^{W_s}[(1-\beta_c)^{l-(m-x+1)}l + \sum_{w=1}^{l-(m-x+1)}(1-\beta_c)^{w-1}\beta_c(w+m-x)] \tag{42}$$

5) A System of Fixed Point Equations: Equations 36-42 together form a system of vector fixed point equations in (β_d, β_c) (it can be observed that β_s is a deterministic function of β_d alone), which can be solved using an iterative procedure until convergence to obtain the attempt rates β_d, β_s, and β_c.

6) Computation of the Average Attempt Rate, β, Over All Backoff Time: The backoff cycle analysis can be used to obtain the long run average attempt rate, β, averaged over all backoff time (irrespective of system state).

To obtain β, note that each backoff cycle contains exactly one attempt by the tagged node, and the backoff counted by the tagged node in the entire backoff cycle contributes towards β. In a backoff cycle starting in state (s,x), the mean backoff counted by the tagged node is clearly $(W_s+1)/2$. Thus, using Markov regenerative analysis, we have

$$\beta = \frac{1}{\sum_{(s,x)}\psi(s,x)\frac{W_s+1}{2}} \tag{43}$$

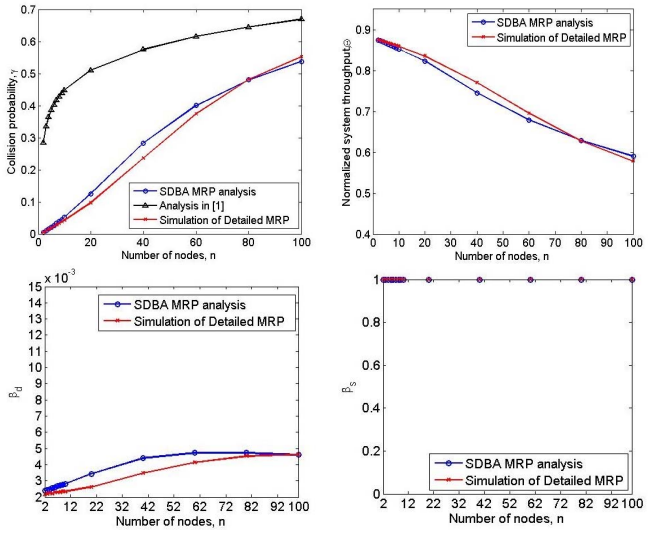

Fig. 10. Zero propagation delay $m = 0$, comparison of SDBA MRP analysis with simulation for various n; backoff sequence ($K = 7$, $b_0 = 1$, $b_k = 3^k b_0$). Note that $\beta_s = 1$ since $b_0 = 1$.

G. Discussion on the Existence and Uniqueness of the Fixed Point

Theorem 1: 1. There exists a fixed point for the system of equations 26-32 in the set $\mathbf{C} = [1/W_K, 1] \times [1/W_K, 1]$.

2. There exists a fixed point for the system of equations 36-42 in the set $\mathbf{C} = [1/W_K, 1] \times [1/W_K, 1]$.

Proof: The proof follows from Brouwer's fixed point theorem. See the techreport [16] for details. ■

We do not have proof of uniqueness of the fixed point. However, in our numerical experiments, the iterations always converged to the same solutions (within a tolerance of 10^{-8}) even when starting with different initial values.

VIII. Model Validation Through Simulations

To validate our analytical model, we performed extensive simulations with a wide range of the number of nodes, n (for $m = 0$ case), and the propagation delay, m (for $n = 2$ case).

For each test case, we used the method of simulating the detailed Markov renewal model, described in Section VI-B, for reasons explained in that section. Throughout the simulations, we use the following parameter values: data packet length 1028 bytes, Rx-to-tx turnaround time $T_o = 10$ μs, PHY rate of 2 Mbps for data packets, and 1 Mbps for control packets. Length of ACK packets, SIFS and DIFS are as in the IEEE 802.11b standard.

To obtain the various measures, namely, $\gamma, \beta_d, \beta_s, \beta_c$ from the simulations, we use their respective definitions introduced in Sections VII-B and VII-E.

The results for the case of $m = 0$ are summarized in Figure 10. For brevity, we have relegated the β_c plots to the Supplementary Material.

Observations:

1) The SDBA MRP analysis predicts the collision probability within an error of about 10% compared to simulations. The mean field analysis, on the other hand, is grossly inaccurate in all the test cases, providing best-case errors of 20-25%.

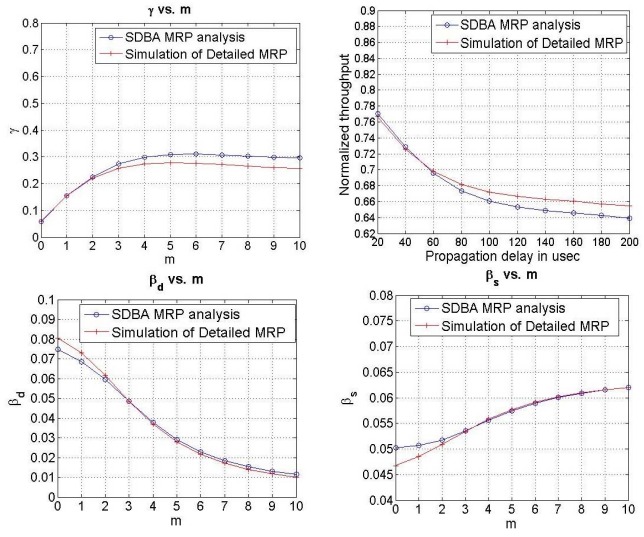

Fig. 11. Scenario (b) in Figure 3, $\Delta = \Delta_r$, varying m; default backoff parameters of IEEE 802.11b. Comparison of the SDBA MRP analysis against simulations.

2) The SDBA MRP analysis also predicts the throughput within an error of at most 2-3%.

3) The errors in the SDBA MRP analysis compared to simulations are at most 10-14% in predicting the attempt rates, β_d, β_s, and β_c. For all test sequences, the qualitative trends in the attempt rates as a function of n are captured by the analysis.

4) The collision probability, γ, increases with the number of nodes, n, as expected.

5) The normalized system throughput, Θ, decreases with increasing n, since collision probability increases.

6) $\beta_s \gg \beta_d$, i.e., the attempt rate is skewed in favor of the successful node, *a reflection of the short term unfairness property*.

7) On an Ubuntu 12.04 platform with 8 GB RAM, i5 processor (clock speed up to 3.2 GHz, 6 MB cache), the running time of the SDBA MRP analysis is several seconds, and that of the stochastic simulation is of the order of several minutes; no multicore optimization was used. It takes up to several hours to run the Qualnet simulation, especially when the short term unfairness is severe. □

For the large propagation delay case, we performed extensive simulations on the topology depicted in Scenario (b), Figure 3, with saturated transmit queues; we assumed equal propagation delay Δ among all nodes (i.e., $\Delta_r = \Delta$), and varied Δ across simulations. We used the default backoff parameters of IEEE 802.11b.

Figure 11 summarizes the results. For brevity, we have relegated the β_c and β plots to the Supplementary Material. Note that while collision probabilities depend only on $m = \lfloor \frac{\Delta}{\sigma} \rfloor$, the propagation delay in integer multiples of slots (see Section VI), throughput depends on the actual ratio $\frac{\Delta}{\sigma}$, since it involves computing the actual lengths of the transmission cycle, and the data duration.

Observations:

1. The relative errors in the approximate analysis compared to simulations are at most 8%, 2-4%, and 2-3% respectively in predicting the collision probability, attempt rates, and throughput, thus validating the accuracy of the analysis. Also, the trend of the collision probability as a function of m is captured well by the approximate analysis.

2. As m increases, β_s monotonically increases, β_d, and β_c monotonically decrease. An intuition behind this follows from the intuitive explanation of the short term unfairness property provided in the discussion at the end of Section V-A.

3. At higher m, $\beta_s \gg \beta_d$, *which is a reflection of the short term unfairness property* demonstrated in Section V-A.

4. As m increases, *the collision probability γ increases at first, but then gradually flattens out*. This is due to the opposing effects on γ of increasing m and stochastically increasing contention window size.

Applications of the Approximate Analysis: Some interesting applications of the approximate SDBA MRP analysis are (i) quantifying the extent of short term unfairness, (ii) tuning slot duration for throughput maximization, and (iii) tuning the backoff sequence to maximize system throughput subject to fairness constraints. Details of these are in the techreport [16].

IX. Conclusion

We have considered a class of single-hop networks with saturated, IEEE 802.11 DCF based transmitters and their receivers, where the systems exhibit short term unfairness. Examples show that short term unfairness arises for several classes of backoff sequences, as well as when the propagation delays among the nodes are large compared to the slot duration. In these cases, the standard fixed point analysis (or simple extensions thereof) does not predict the system performance well. We concluded from these examples that the inability of the standard fixed point model to capture the performance in such cases is due to the *state-independent* attempt rate assumption. We then developed a novel computationally tractable, yet accurate, approximate analysis using state-dependent Bernoulli attempt processes with a small number of additional parameters, yielding an overall Markov renewal process (SDBA MRP). Our analysis is numerically quite accurate, and captures the qualitative trends in collision probability and throughput. In addition to providing a tool for performance prediction, our analysis will also be useful for MAC parameter selection for particular performance profiles.

References

[1] G. Bianchi, "Performance analysis of the IEEE 802.11 distributed coordination function," *IEEE J. Sel. Areas Commun.*, vol. 18, no. 3, pp. 535–547, Mar. 2000.

[2] A. Kumar, E. Altman, D. Miorandi, and M. Goyal, "New insights from a fixed-point analysis of single cell IEEE 802.11 WLANs," *IEEE/ACM Trans. Netw.*, vol. 15, no. 3, pp. 588–601, Jun. 2007.

[3] V. Ramaiyan, A. Kumar, and E. Altman, "Fixed point analysis of single cell IEEE 802.11e WLANs: Uniqueness and multistability," *IEEE Trans. Netw.*, vol. 16, no. 5, pp. 1080–1093, Oct. 2008.

[4] B. Raman and K. Chebrolu, "Experiences in using WiFi for rural Internet in India," *IEEE Commun. Mag.*, vol. 45, no. 1, pp. 104–110, Jan. 2007.

[5] G. W. Wong and R. W. Donaldson, "Improving the QoS performance of EDCF in IEEE 802.11e wireless LANs," in *Proc. IEEE PACRIM*, Aug. 2003, pp. 392–396.

[6] A. Jindal and K. Psounis, "The achievable rate region of 802.11-scheduled multihop networks," *IEEE/ACM Trans. Netw.*, vol. 17, no. 4, pp. 1118–1131, Aug. 2009.

[7] B. Nardelli and E. W. Knightly, "Closed-form throughput expressions for CSMA networks with collisions and hidden terminals," in *Proc. IEEE INFOCOM*, Mar. 2012, pp. 2309–2317.
[8] I. Tinnirello and G. Bianchi, "Rethinking the IEEE 802.11e EDCA performance modeling methodology," *IEEE/ACM Trans. Netw.*, vol. 18, no. 2, pp. 540–553, Apr. 2010.
[9] M. Garetto, J. Shi, and E. W. Knightly, "Modeling media access in embedded two-flow topologies of multi-hop wireless networks," in *Proc. ACM MobiCom*, 2005, pp. 200–214.
[10] F.-J. Simo-Reigadas, A. Martínez-Fernandez, F.-J. Ramos-López, and J. Seoane-Pascual, "Modeling and optimizing IEEE 802.11 DCF for long-distance links," *IEEE Trans. Mobile Comput.*, vol. 9, no. 6, pp. 881–896, Jun. 2010.
[11] *QualNet Webpage*. Accessed: Sep. 18, 2017. [Online]. Available: http://web.scalable-networks.com/content/qualnet
[12] C. Vlachou, A. Banchs, J. Herzen, and P. Thiran, "On the MAC for power-line communications: Modeling assumptions and performance tradeoffs," in *Proc. IEEE ICNP*, Apr. 2014, pp. 456–467.
[13] M. Benaïm and J.-Y. Le Boudec, "A class of mean field interaction models for computer and communication systems," *Perform. Eval.*, vol. 65, nos. 11–12, pp. 823–838, 2008.
[14] F. D. Ohrtman and K. Roedar, *Wi-Fi Handbook: Building 802.11b Wireless Networks*. New York, NY, USA: McGraw-Hill, 2003.
[15] P. Sprent and N. C. Smeeton, *Applied Nonparametric Statistical Methods*. Boca Raton, FL, USA: Chapman & Hall, 2007.
[16] A. Bhattacharya and A. Kumar. (Jul. 2016). "Analytical modeling of IEEE 802.11 type CSMA/CA networks with short term unfairness." [Online]. Availble: https://arxiv.org/abs/1607.07021
[17] G. Bianchi and I. Tinnirello, "Remarks on IEEE 802.11 DCF performance analysis," *IEEE Commun. Lett.*, vol. 9, no. 8, pp. 765–767, Aug. 2005.
[18] V. G. Kulkarni, *Modeling and Analysis of Stochastic Systems*. London, U.K.: Chapman & Hall, 1995.

Abhijit Bhattacharya received the M.E. and the Ph.D. degrees in telecommunication engineering from the Indian Institute of Science, Bangalore, India, in 2010 and 2016, respectively. From 2010 to 2011, he was with Cisco Systems Pvt. Ltd., India. He is currently a Senior Systems Engineer with Qualcomm Research India. His research interests include the optimal design of wireless networks with various performance constraints and energy constraints, the performance modeling, analysis, and optimal control of wireless networks, and the application of machine learning tools for field-interactive and adaptive network design.

Anurag Kumar (F'06) received the B.Tech. degree in electrical engineering from IIT Kanpur, Kanpur, India, and the Ph.D. degree in electrical engineering from Cornell University. He was with Bell Labs, Holmdel, NJ, USA, for over six years. He is currently a Professor with the ECE Department, Indian Institute of Science, Bangalore, India, where he is also the Director. His research interests include communication networking and wireless networking. He is a fellow of the Indian National Science Academy, the Indian National Academy of Engineering, and the Indian Academy of Sciences. He was an Associate Editor of the IEEE/ACM TRANSACTIONS ON NETWORKING and the IEEE COMMUNICATIONS SURVEYS AND TUTORIALS.